Siderophore-Mediated Cargo Delivery to the Cytoplasm of Escherichia coli and Pseudomonas aeruginosa: Syntheses of Monofunctionalized Enterobactin Scaffolds and Evaluation of Enterobactin-Cargo Conjugate Uptake

Siderophore-Mediated Cargo Delivery to the Cytoplasm of *Escherichia coli* and *Pseudomonas aeruginosa*: Syntheses of Monofunctionalized Enterobactin Scaffolds and Evaluation of Enterobactin-Cargo Conjugate Uptake

Tengfei Zheng, Justin L. Bullock, and Elizabeth M. Nolan*

Department of Chemistry, Massachusetts Institute of Technology, Cambridge, MA 02139

*Corresponding author: lnolan@mit.edu

Phone: 617-452-2495

Fax: 617-324-0505

Abstract

The design and syntheses of monofunctionalized enterobactin (Ent, L- and D-isomers) scaffolds where one catecholate moiety of enterobactin houses an alkene, aldehyde, or carboxylic acid moiety at the C5 position are described. These molecules are key precursors to a family of ten enterobactin-cargo conjugates presented in this work, which were designed to probe the extent to which the Gram-negative ferric enterobactin uptake and processing machinery recognizes, transports, and utilizes derivatized enterobactin scaffolds. A series of growth recovery assays employing enterobactin-deficient *E. coli* ATCC 33475 (*ent*-) revealed that six conjugates based on L-Ent having relatively small cargos promoted *E. coli* growth under iron-limiting conditions whereas negligible-to-no growth recovery was observed for four conjugates with relatively large cargos. No growth recovery was observed for the enterobactin receptor deficient strain of *E. coli* H1187 (*fepA-) or* the enterobactin esterase-deficient derivative of *E. coli* K-12 JW0576 *(fes*-), or when the D-isomer of enterobactin was employed. These results demonstrate that the *E. coli* ferric enterobactin transport machinery identifies and delivers select cargo-modified scaffolds to the *E. coli* cytoplasm. *Pseudomonas aeruginosa* PAO1 K648 (*pvd*-, *pch*-) exhibited greater promiscuity than that of *E. coli* for the uptake and utilization of the enterobactin-cargo conjugates, and growth promotion was observed for eight conjugates under iron-limiting conditions. Enterobactin may be utilized for delivering molecular cargos via its transport machinery to the cytoplasm of *E. coli* and *P. aeruginosa* thereby providing a means to overcome the Gram-negative outer membrane permeability barrier.

Introduction

Siderophores are low-molecular-weight high-affinity Fe(III) chelators that are biosynthesized and exported by bacteria, fungi, and plants during periods of nutrient limitation for acquiring this essential metal ion from the extracellular milieu.[1,2] Both naturally-occurring and synthetic siderophore mimics are useful for bioremediation,[3] iron chelation therapies,[4,5] antibiotic drug-delivery strategies,[6-14] Fe(III) detection,[15-18] protein identification,[19] and pathogen capture.[20, 21] These types of applications benefit from or require siderophores amenable to facile and site-specific synthetic modification. In this work, we expand the current toolkit of site-specifically modifiable siderophore scaffolds to include triscatecholate enterobactin, and we report that various synthetic enterobactin-cargo conjugates are actively transported to the cytoplasm of the Gram-negative bacterial species *Escherichia coli* and *Pseudomonas aeruginosa* by the enterobactin uptake machinery.

Enterobactin (Ent, **1**, Figure 1A) is a canonical siderophore biosynthesized by Gram-negative species of *Enterobacteriaceae* that include *Escherichia coli*, *Salmonella*, and *Klebsiella*.[22] Decades of exploration pertaining to enterobactin biosynthesis and coordination chemistry, in addition to investigations of the proteins involved in its cellular transport and processing, provide a detailed molecular and physiological understanding of how this chelate contributes to bacterial iron homeostasis and colonization.[22] The enterobactin synthetase is comprised of four proteins, EntBDEF, and is responsible for the production of enterobactin from L-serine and 2,3-dihydroxybenzoic acid (DHB).[23] Following biosynthesis, Ent is exported into the extracellular space where it scavenges Fe(III). Enterobactin coordinates Fe(III) by its three catecholate groups with $K_a \sim 10^{49}$ M^{-1}.[24] In *E. coli*, the outer membrane transporter FepA (and to a lesser extent Cir and Fiu) recognizes and binds ferric enterobactin with sub-nanomolar affinity,[25,26] and provides periplasmic entry where the siderophore forms a complex with the periplasmic binding protein FepB.[27] Subsequently, $[Fe(Ent)]^{3-}$ is transported into the cytosol, which requires the action of ExbBD, TonB, and FepCDG, the latter of which constitute the inner-membrane ATP-binding cassette (ABC) transporter system (Figure 1B).[28-32] Fes, the cytosolic

enterobactin esterase, catalyzes the hydrolysis of the $[Fe(Ent)]^{3-}$ macrolactone,[33] and the ferric reductase YgjH may subsequently assist in Fe(III) release such that the metal ion can be used metabolically.[34] Several pathogenic Gram-negative species harbor gene clusters (e.g. *iroA*, MccE492) responsible for post-assembly line modifications of the enterobactin scaffold to provide the salmochelins.[33,35-38] Salmochelins are a family of glucosylated enterobactin derivatives where the sugar moieties are attached to the C5 position of one or more catecholate rings (e.g. MGE **2** and DGE **3**, Figure 1A).[39]

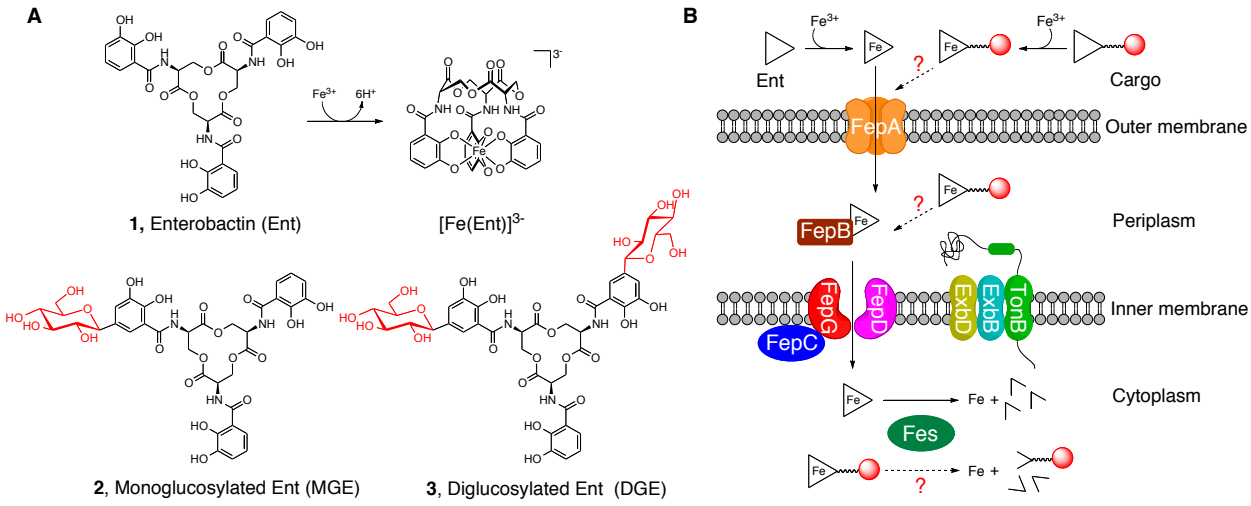

Figure 1. Siderophores and siderophore transport machinery relevant to this work. (A) Structures of enterobactin **1** and the salmochelins MGE **2** and DGE **3**. (B) Cartoon depiction of the enterobactin transport and processing machinery in *E. coli*.

Gram-negative bacteria have an outer membrane that serves as a permeability barrier and prevents cellular entry of many molecules, including antibiotics (e.g. vancomycin). Siderophore uptake machinery provides one route to overcome this permeability barrier,[6-14] and enterobactin and its transporter FepA have been identified as a desirable siderophore/receptor pair for cargo delivery to Gram-negative bacterial species.[13,37] FepA-mediated uptake of the ribosomal peptide antibiotics colicin B[40] and MccE492m,[41] in addition to bacteriophage,[42]

indicates that this receptor has the capacity to transport large molecules. Moreover, the catecholate siderophore transporters of *E. coli* (e.g. Fiu, Cir) recognize synthetic catechol-modified β-lactam antibiotics;[43-46] these serendipitous observations motivated early "Trojan horse" delivery strategies. Indeed, small-molecule antibiotics appended to siderophore-inspired di- and tricatecholate platforms have been evaluated for antibacterial activity with mixed results.[47-51] Most recently, amoxicillin and ampicillin, β-lactam antibiotics that act in the periplasm and target bacterial cell wall biosynthesis, were covalently linked to a tripodal catecholate platform and remarkably afforded ca. 10^2- to 10^3-fold enhanced activity against *P. aeruginosa* PAO1 compared to the free drug.[49]

The ability of FepABCDG and the TonB-ExbB-ExbD system of *E. coli*, as well as the enterobactin transport machinery of other bacterial species, to recognize and provide cytosolic transport of unnatural cargo appended to the native ligand remains unexplored. Enterobactin exhibits C_3 symmetry and houses no unique functional group for site-specific synthetic modification. Total syntheses of enterobactin,[52-56] hydrolytically stable enterobactin analogs,[57-60] and salmochelins[61] have been reported. To the best of our knowledge, no enterobactin scaffold housing a site-specific synthetic handle has been presented. Such scaffolds are a pre-requisite for employing enterobactin in a variety of paradigms that include cargo delivery, iron and siderophore detection, and bacterial capture.

Herein we present a family of ten enterobactin-cargo conjugates that are based on a monofunctionalized enterobactin scaffold. Inspired by the salmochelins, we have derivatized enterobactin at the C5 position of the catecholate, which provides a point for site-specific modification without compromising the Fe(III)-binding groups or the macrolactone (Figure 2). Moreover, we report that the ferric enterobactin uptake machineries of *Escherichia coli* and *Pseudomonas aeruginosa* PAO1 deliver enterobactin-derivatized cargo to the cytoplasm of both species under iron deficient conditions, and that cargo size is an important and species/strain-specific parameter to evaluate in enterobactin conjugate design.

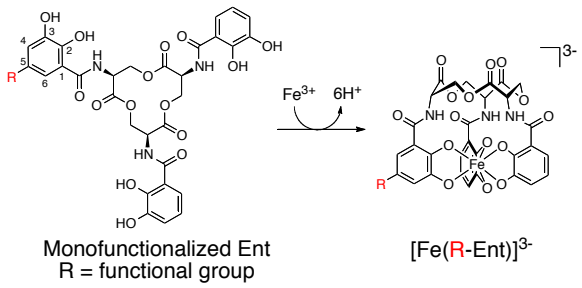

Figure 2. Enterobactin substituted at the C5 position.

Experimental

Reagents. Dimethylformamide (DMF) and dichloromethane (CH_2Cl_2) were dried over 4 Å molecular sieves or by using a VAC solvent purification system (Vacuum Atmospheres). Anhydrous dimethyl sulfoxide (DMSO) was purchased from Sigma-Aldrich and used as received. The triserine lactone **4** and its D-isomer **5** were synthesized according to a literature procedure.[55] 2,3-Bis(benzyloxy)benzoic acid **6**,[62] vancomycin-alkyne **7**,[63] and *tert*-butyl (2-oxo-2-(prop-2-yn-1-ylamino)ethyl)carbamate **8**,[63] were synthesized according to literature procedures. L-Ent **1** and its D-isomer **9** were synthesized as reported elsewhere.[55,56] *Tert*-butyl 3-(2-(2-(2-aminoethoxy)ethoxy)ethoxy)propanoate **10** was purchased from BOC Sciences (Shirley, NY), 11-azido-3,6,9-trioxaundecan-1-amine **11** was purchased from Fluka, 6-((*tert*-butyoxycarbonyl)amino)hexanoic acid **12** was purchased from Advanced Chem Tech, and Fmoc-PEG-CO_2H **13** was purchased from Chem-Impex International, Inc. The syntheses of the PEG-derivatized cargos **14-18** are provided as Supporting Information. Methyl-5-allyl-3-methoxysalicylate **19** was obtained from Sigma Aldrich. All other chemicals were purchased from Sigma-Aldrich, Alfa Aesar, or TCI in the highest available purity and used as received.

General Synthetic Materials and Methods. EMD TLC silica gel 60 F_{254} plates were used for analytical thin-layer chromatography. EMD PLC silica gel 60 F_{254} plates of 1-mm thickness were used for preparative TLC. Zeoprep 60HYD silica gel (40-63 μm) obtained from Zeochem was used for flash chromatography. ^{1}H, ^{19}F, and ^{13}C NMR spectra were collected on a Varian

300 or 500 MHz spectrophotometer, which were operated at ambient probe temperature (283 K) and housed in the Department of Chemistry Instrumentation Facility. The ^{1}H and ^{13}C NMR spectra were referenced to internal standards and ^{19}F spectra were referenced to an external CF_3Cl standard. An Avatar FTIR instrument was used to acquire IR spectra. Optical absorption spectra were recorded on an Agilent 8453 diode array spectrophotometer (1-cm quartz cuvettes, Starna). General methods for high performance liquid chromatography and mass spectrometry, ^{1}H and ^{13}C NMR spectra, and IR spectroscopic data are provided as Supporting Information.

Methyl-5-allyl-2,3-dihydroxybenzoate (20). Methyl-5-allyl-3-methoxysalicylate (**19**, 2.22 g, 10.0 mmol) and anhydrous *N*,*N*-diisopropylethylamine (DIPEA, 1.94 g, 15.0 mmol) were dissolved in 125 mL of dry CH_2Cl_2 and stirred at rt for five min. The solution was cooled to −78 °C in an acetone/dry ice bath, and boron tribromide (BBr_3, 1M solution in CH_2Cl_2, 30 mL, 30 mmol) was added slowly over ca. 10 min via a syringe to afford a yellow solution. The reaction was stirred at −78 °C for 1 h, warmed to −30 °C over the course of 1 h, and subsequently warmed to rt and stirred for another 4.5 h. Water (200 mL) was added slowly to quench the reaction, and the organic phase was washed with saturated aqueous potassium bicarbonate (K_2CO_3, 3 x 100 mL). The organic phase was dried over sodium sulfate (Na_2SO_4), and the solvent was removed under reduced pressure to afford a brown oil. Flash chromatography on silica gel with a solvent gradient (100% hexanes to 20% EtOAc/hexanes) gave the product as a white solid (1.09 g, 53%). TLC R_f =0.5 (silica, CH_2Cl_2); mp = 55-56 ^{o}C. ^{1}H NMR ($CDCl_3$, 500 MHz), δ 3.29 (2H, d, *J* = 7.0 Hz), 3.95 (3H, s), 5.05-5.10 (2H, m), 5.80 (1H, s), 5.91 (1H, m), 6.97 (1H, s), 7.18 (1H, s), 10.76 (1H, s). ^{13}C NMR ($CDCl_3$, 125 MHz), δ 39.4, 52.3, 111.9, 116.0, 119.8, 120.4, 131.1, 137.0, 144.8, 147.2, 170.7. HRMS (DART): $[M+Na]^+$ *m/z* calcd., 231.0628; found, 231.0637.

5-Allyl-2,3-bis(benzyloxy)benzoic acid (21). Alkene **20** (2.18 g, 10.5 mmol), benzyl bromide (10.8 g, 60.3 mmol), and K_2CO_3 (24.5 g, 17.8 mmol) were combined in 200 mL of acetone at rt. The reaction was refluxed under N_2 for 16 h, which provided a yellow solution with

white solids, and the mixture was cooled to rt and filtered. The filtrate was concentrated under reduced pressure to afford a yellow oil. The oil was dissolved in a 375-mL mixture of 4:1 MeOH / 5 M NaOH (aq). The resulting solution was refluxed for 3.5 h and concentrated under reduced pressure to afford a white-yellow oil. Water (300 mL) was added to the oil, and the aqueous phase was washed with hexanes (4 x 100 mL). The pH of the aqueous phase was adjusted to ca. 1 by addition of 12 M HCl and the product precipitated as a white solid. A 100-mL portion of CH_2Cl_2 was added, and the resulting mixture was partitioned. The aqueous phase was extracted with additional CH_2Cl_2 (2 x 100 mL) and the combined organic layers were dried over Na_2SO_4 and concentrated under reduced pressure to yield **21** as a white solid (3.91 g, 99%). TLC R_f = 0.55 (silica, 100% CH_2Cl_2); mp = 135-136 ^oC. ^1H NMR ($CDCl_3$, 300 MHz), δ 3.38 (2H, d, J = 6.6 Hz), 5.06-5.14 (2H, m), 5.17 (2H, s), 5.22 (2H, s), 5.92 (1H, m), 7.09 (1H, d, J = 2.1 Hz), 7.31-7.50 (10H, m), 7.58 (1H, m). ^{13}C NMR ($CDCl_3$, 125 MHz), δ 39.6, 71.4, 76.9, 116.7, 119.3, 122.6, 123.9, 127.8, 128.4, 128.7, 128.7, 129.1, 129.2, 134.8, 135.8, 136.2, 137.2, 145.5, 151.2, 165.6. HRMS (DART): $[M-H]^-$ *m/z* calcd., 373.1445; found, 373.1439.

(*E*)-2,3-Bis(benzyloxy)-5-(prop-1-en-1-yl)benzoic acid (22). A 30-mL portion of methanol (MeOH) was degassed with N_2 for 4 h at rt and **21** (750 mg, 2.00 mmol) was subsequently added. The mixture was stirred at rt until **21** dissolved and $PdCl_2$ (58 mg, 0.32 mmol) was added to give a cloudy brown solution. The reaction was stirred at rt for 24 h and filtered. The filtrate was concentrated and purified by column chromatography using silica gel (1:4:5 EtOAc/hexanes/CH_2Cl_2) to yield **22** as a light yellow solid (666 mg, 89%). TLC R_f = 0.4 (40% EtOAc/hexanes); mp = 140-142 ^oC. ^1H NMR ($CDCl_3$, 300 MHz), δ 1.88-1.90 (3H, m), 5.19 (2H, s), 5.23 (2H, s), 6.25 (1H, dq, J = 15.9, 6.0 Hz), 6.32-6.38 (1H, m), 7.22 (1H, d, J = 2.1 Hz), 7.32-7.51 (10H, m), 7.69 (1H, d, J = 2.1 Hz). ^{13}C NMR ($CDCl_3$, 125 MHz), δ 18.3, 71.4, 77.0, 115.8, 121.6, 122.7, 127.4, 127.7, 128.4, 128.7, 129.1, 129.2, 129.3, 134.7, 135.0, 135.9, 145.7, 151.3, 165.5. HRMS (DART): $[M-H]^-$ *m/z* calcd., 373.1445; found, 373.1457.

***N,N'*-((3S,7S,11S)-11-(2,3-Bis(benzyloxy)-5-((E)-prop-1-en-1-yl)benzamido)-2,6,10-trioxo-1,5,9-trioxacyclododecane-3,7-diyl)bis(2,3-bis(benzyloxy)benzamide) (23).** Trilactone **4**

(740 mg, 2.00 mmol) and DIPEA (2.58 g, 20 mmol) were mixed in dry DMSO (8 mL) and stirred for 10 min at rt to give a clear solution. PyAOP (3.13 g, 6.07 mmol), **22** (748 mg, 2.00 mmol) and **6** (1.00 g, 2.99 mmol) were dissolved in dry DMSO (10 mL) and added to the solution containing **4**, and the reaction turned yellow and became orange after stirring for 2 h at rt. The orange solution was mixed with EtOAc (50 mL) and water (50 mL) and partitioned. The organic phase was washed with brine (3 x 50 mL), dried over Na_2SO_4, and concentrated to afford a yellow oil. Flash chromatography on silica gel with a solvent gradient (10% EtOAc/hexanes to 55% EtOAc/hexanes) yielded the product as a white foam (931 mg, 37%). TLC R_f = 0.3 (50% EtOAc/hexanes); mp = 100-102 ^oC (decomp). ^1H NMR ($CDCl_3$, 300 MHz), δ 1.88-1.91 (3H, m), 4.01-4.11 (3H, m), 4.16-4.22 (3H, m), 4.91-4.98 (3H, m), 5.03-5.19 (12H, m), 6.17-6.40 (2H, m), 7.10-7.47 (32H, m), 7.66-7.71 (3H, m), 8.51-8.53 (3H, m). ^{13}C NMR ($CDCl_3$, 125 MHz), δ 18.2, 40.6, 51.2, 63.9, 70.9, 76.0, 76.1, 114.2, 117.3, 120.4, 122.8, 124.1, 125.7, 126.1, 126.3, 127.4, 127.5, 127.9, 128.0, 128.2, 128.4, 128.4, 128.4, 128.7, 128.7, 129.6, 134.1, 135.8, 135.8, 136.0, 136.0, 145.5, 146.7, 151.4, 151.4, 164.7, 168.8, 168.8. HRMS (DART): $[M+H]^+$ *m/z* calcd., 1250.4645; found, 1250.4653.

***N,N'*-((3S,7S,11S)-11-(2,3-Bis(benzyloxy)-5-formylbenzamido)-2,6,10-trioxo-1,5,9-trioxacyclododecane-3,7-diyl)bis(2,3-bis(benzyloxy)benzamide) (24).** A portion of compound **23** (285 mg, 0.228 mmol) was dissolved in 1,4-dioxane (9 mL) at rt, and water (3 mL) was added to give a colorless solution. Osmium tetraoxide (OsO_4, 68 μL of 2.5% wt solution in 2-methyl-2 propanol, 6.7 μmol) was added and the reaction was stirred for 0.5 h at rt, which afforded a light brown solution. Sodium periodate ($NaIO_4$, 76.5 mg, 0.570 mmol) was then added and the reaction was stirred for another 2 h at rt. The suspension was partitioned in water (20 mL) and EtOAc (50 mL). The organic phase was washed with 0.1 M sodium thiosulfate ($Na_2S_2O_3$, 3 x 20 mL) and brine (2 x 20 mL), and dried over Na_2SO_4. Flash chromatography on silica gel with a solvent gradient (20% EtOAc/hexanes to 65% EtOAc/hexanes) yielded the product as white solid (165 mg, 58%). TLC R_f = 0.6 (70% EtOAc/hexanes); mp = 74 ^oC (decomp). ^1H NMR ($CDCl_3$, 300 MHz), δ 4.03-4.11 (3H, m), 4.18-4.26 (3H, m), 4.90-4.96 (3H,

m), 5.05-5.28 (12H, m), 7.09-7.44 (31H, m), 7.65-7.67 (2H, m), 8.14-8.15 (1H, m), 8.46-8.52 (3H, m), 9.86 (1H, s). ^{13}C NMR ($CDCl_3$, 125 MHz), δ 51.4, 51.4, 51.7, 64.1, 64.2, 71.0, 71.2, 76.2, 76.2, 76.5, 113.1, 117.3, 117.4, 122.9, 123.0, 124.2, 126.2, 126.3, 126.5, 127.5, 127.6, 127.8, 128.1, 128.3, 128.4, 128.4, 128.5,128.5, 128.5, 128.6, 128.8, 128.9, 132.1, 135.2, 135.3, 135.9, 135.9, 136.0, 146.7, 146.8, 151.5, 151.5, 151.7, 152.2, 163.7, 164.9, 164.9, 168.7, 168.9, 169.1, 190.6. HRMS (DART): $[M+H]^+$ *m/z* calcd., 1238.4287; found, 1238.4279.

3,4-Bis(benzyloxy)-5-(((3S,7S,11S)-7,11-bis(2,3-bis(benzyloxy)benzamido)-2,6,10-trioxo-1,5,9-trioxacyclododecan-3-yl)carbamoyl)benzoic acid (25). A portion of **24** (112 mg, 0.0903 mmol) was dissolved in 1,4-dioxane (3 mL) at rt. Sulfamic acid (NH_3SO_3, 15.8 mg, 0.162 mmol) was dissolved in water (0.75 mL) and added to the dioxane solution. Sodium chlorite ($NaClO_2$, 14.7 mg, 0.163 mmol) dissolved in 0.2 mL of water and the resulting solution was added to the reaction over the course of 10 min, and the reaction turned yellow. After stirring for 0.5 h at rt, the reaction was partitioned in water (10 mL) and EtOAc (20 mL), the aqueous phase was extracted with EtOAc (2 x 10 mL), and the combined organic phases were dried over Na_2SO_4. Flash chromatography on silica gel with a solvent gradient (CH_2Cl_2 to 10% MeOH/CH_2Cl_2) yielded the product as white solid (87 mg, 76%). TLC R_f = 0.5 (10% MeOH/ CH_2Cl_2); mp = 128-129 ^{o}C (decomp). ^{1}H NMR ($CDCl_3$, 500 MHz), δ 4.05-4.08 (3H, m), 4.22-4.25 (3H, m), 4.93-4.98 (3H, m), 5.06-5.25 (12H, m), 7.06-7.47 (31H, m), 7.67-7.69 (2H, m), 7.86 (1H, s), 8.44-8.47 (2H, m), 8.54-8.57 (2H, m). ^{13}C NMR ($CDCl_3$, 125 MHz), δ 51.4, 51.5, 51.6, 64.1, 71.1, 71.2, 76.2, 76.4, 117.5, 117.6, 123.0, 124.2, 125.4, 125.6, 126.2, 127.5, 127.6, 127.8, 128.1, 128.3, 128.4, 128.4, 128.5, 128.6, 128.7, 128.8, 128.9, 135.4, 135.6, 135.9, 136.1, 146.8, 150.7, 151.4, 151.5, 164.1, 165.0, 168.8, 168.9, 169.0, 169.3. HRMS (DART): $[M+H]^+$ *m/z* calcd., 1254.4230; found, 1254.4204.

Enantiomers 26-28. The D-isomers of the enterobactin alkene **23**, aldehyde **24**, and acid **25** were synthesized as described for the L-isomers except that triserine lactone **5** was employed instead of **4**. The synthetic procedures and characterization are provided as Supporting Information.

***Tert*-butyl(1-(3-(((3S,7S,11S)-7,11-bis(2,3-dihydroxybenzamido)-2,6,10-trioxo-1,5,9-trioxacyclododecan-3-yl)carbamoyl)-4,5-dihydroxyphenyl)-1-oxo-5,8,11-trioxa-2-azatridecan-13-yl)carbamate (29).** Compound **25** (50 mg, 40 ∫mol), PyAOP (34 mg, 60 ∫mol) and DIPEA (15.2 ∫L, 160 ∫mol) were mixed in 2 mL of dry CH_2Cl_2 at rt. A portion of **7** (15 mg, 48 ∫mol) was then added and the resulting yellow solution was stirred for 4 h at rt. The crude reaction was washed with 0.01N HCl (2 x 10 mL), dried over Na_2SO_4, and concentrated. The benzyl-protected product was purified by preparative TLC (10% MeOH/CH_2Cl_2) and obtained as a white viscous solid (46 mg, 75%). TLC R_f = 0.7 (10% MeOH/CH_2Cl_2). ^{1}H NMR ($CDCl_3$, 500 MHz), δ 1.42 (9H, s), 3.27-3.28 (2H, m), 3.50-3.52 (2H, m), 3.59-3.66 (12H, m), 4.02-4.07 (3H, m), 4.15-4.18 (3H, m), 4.90-4.94 (3H, m), 5.03-5.20 (12H, m), 7.10-7.45 (36H, m), 7.65-7.67 (2H, m), 7.85-7.85 (1H, m), 7.99 (1H, bs), 8.49-8.54 (3H, m). ^{13}C NMR ($CDCl_3$, 125 MHz), δ 28.3, 39.9, 40.2, 51.3, 51.4, 63.9, 64.1, 69.7, 70.0, 70.2, 70.3, 70.4, 71.1, 71.2, 76.2, 76.3, 79.0, 116.7, 117.5, 120.3, 123.0, 124.2, 125.4, 126.1, 126.2, 127.6, 127.6, 127.8, 128.2, 128.3, 128.4, 128.4, 128.4, 128.5, 128.6, 128.6, 128.7, 128.8, 128.8, 129.0, 130.2, 135.4, 135.7, 135.9, 135.9, 136.1, 146.8, 146.9, 149.0, 151.5, 151.8, 155.9, 164.2, 164.8, 164.9, 165.8, 168.9, 169.0, 169.1. HRMS (ESI): $[M+Na]^+$ *m/z* calcd., 1550.5942; found, 1550.5977.

This benzyl-protected product was dissolved in 2 mL of 1:1 EtOAc/EtOH, the reaction flask was purged with N_2, and 45 mg Pd/C (10% wt) was added. The reaction was stirred under H_2 (1 atm) for 6 h at rt, and the Pd/C was removed by centrifugation (13,000 rpm, 10 min). The clear supernatant was decanted, concentrated, and re-dissolved in a 4:2:1 mixture of 1,4-dioxane/H_2O/MeOH, and purified by semi-preparative HPLC (20% B for 5 min followed by 20-70% B over 15 min, 4 mL/min). The product eluted at 15.8 min and was lyophilized to give **29** as white solid (15 mg, 50%). The analytical HPLC trace of the purified product is reported as Supporting Information. HRMS (ESI): $[M+Na]^+$ *m/z* calcd., 1010.3125; found, 1010.3173.

***N*^{3}-((3S,7S,11S)-7,11-Bis(2,3-dihydroxybenzamido)-2,6,10-trioxo-1,5,9-trioxacyclododecan-3-yl)-*N*^{1}-(1-cyclohexyl-1-oxo-5,8,11-trioxa-2-azatridecan-13-yl)-4,5-dihydroxyisophthalamide (30).** Compound **30** was synthesized as described for **29** except

that **14** (13.6 mg, 45.0 ⌠mol) was used instead of **7**. After purification by preparative TLC (10% MeOH/CH_2Cl_2), the benzyl-protected precursor of **30** was obtained as a white viscous solid (37 mg, 60%). TLC R_f = 0.6 (10% MeOH/CH_2Cl_2). ^{1}H NMR ($CDCl_3$, 500 MHz), δ 1.17-1.21 (3H, m), 1.37-1.43 (2H, m), 1.62-1.63 (1H, m), 1.72-1.74 (2H, m), 1.78-1.81 (2H, m), 2.00-2.06 (1H, m), 3.39-3.42 (2H, m), 3.51-3.53 (2H, m), 3.59-3.61 (2H, m), 3.64-3.65 (10H, m), 4.01-4.06 (3H, m), 4.13-4.17 (3H, m), 4.88-4.93 (3H, m), 5.04-5.21 (12H, m), 6.23-6.25 (1H, m), 7.09-7.45 (35H, m), 7.64-7.66 (2H, m), 7.86 (1H, d, J = 2.0 Hz), 8.02 (1H, d, J = 2.0 Hz), 8.49-8.54 (3H, m). ^{13}C NMR ($CDCl_3$, 125 MHz), δ 25.6, 29.5, 38.8, 40.0, 45.3, 51.3, 51.4, 63.9, 64.1, 69.8, 69.8, 70.0, 70.3, 70.4, 70.4, 71.2, 71.2, 76.2, 76.3, 116.8, 117.5, 120.4, 123.0, 124.3, 125.4, 126.1, 126.2, 127.6, 127.6, 127.9, 128.2, 128.3, 128.4, 128.4, 128.5, 128.5, 128.6, 128.6, 128.8, 128.8, 128.9, 129.0, 130.1, 135.4, 135.7, 135.9, 136.0, 136.1, 146.8, 146.9, 149.1, 151.6, 151.8, 164.3, 164.9, 164.9, 165.8, 168.9, 169.0, 169.1, 176.2. HRMS (ESI): $[M+Na]^+$ *m/z* calcd., 1560.6150; found, 1560.6269. Compound **30** was purified by semi-preparative HPLC (20% B for 5 min followed by 20-70% B over 15 min, 4 mL/min). The product eluted at 15.1 min and was obtained as white solid (20 mg, 58%). The analytical HPLC trace of the purified product is reported as Supporting Information. HRMS (ESI): $[M+Na]^+$ *m/z* calcd., 1020.3333; found, 1020.3346.

***N*^{3}-((3R,7R,11R)-7,11-Bis(2,3-dihydroxybenzamido)-2,6,10-trioxo-1,5,9-trioxacyclododecan-3-yl)-*N*^{1}-(1-cyclohexyl-1-oxo-5,8,11-trioxa-2-azatridecan-13-yl)-4,5-dihydroxyisophthalamide (31).** Compound **31** was synthesized as described for **30** except that **28** (36 mg, 29 ⌠mol) was used instead of **25**. After purification by preparative TLC (10% MeOH/CH_2Cl_2), the benzyl-protected precursor of **31** was obtained as a white oily solid (29 mg, 65%). TLC R_f = 0.6 (10% MeOH/CH_2Cl_2). ^{1}H NMR ($CDCl_3$, 500 MHz), δ 1.17-1.25 (3H, m), 1.38-1.44 (2H, m), 1.63 (1H, m), 1.72-1.81 (4H, m), 2.01-2.06 (1H, m), 3.40-3.41 (2H, m), 3.39-3.42 (2H, m), 3.51-3.53 (2H, m), 3.58-3.65 (12H, m), 4.01-4.06 (3H, m), 4.13-4.16 (3H, m), 4.87-4.95 (3H, m), 5.03-5.21 (12H, m), 6.22-6.23 (1H, m), 7.09-7.45 (35H, m), 7.65-7.66 (2H, m), 7.86 (1H, s), 8.02 (1H, s), 8.49-8.54 (3H, m). ^{13}C NMR ($CDCl_3$, 125 MHz), δ 25.6, 29.5, 38.8, 40.0, 45.3, 51.3, 51.4, 63.9, 64.1, 69.8, 69.8, 70.0, 70.3, 70.4, 70.4, 71.2, 71.2, 76.2, 76.3, 116.8, 117.5, 120.4, 123.0, 124.3,

125.4, 126.1, 126.2, 127.6, 127.6, 127.9, 128.2, 128.3, 128.4, 128.4, 128.5, 128.5, 128.6, 128.6, 128.8, 128.8, 128.9, 129.0, 130.1, 135.4, 135.7, 135.9, 136.0, 136.1, 146.8, 146.9, 149.1, 151.6, 151.8, 164.3, 164.9, 164.9, 165.8, 168.9, 169.0, 169.1, 176.2. HRMS (ESI): $[M+Na]^+$ *m/z* calcd., 1560.6150; found, 1560.6141. Compound **31** was purified by semi-preparative HPLC (20% B for 5 min followed by 20-70% B over 15 min, 4 mL/min). The product eluted at 14.8 min and was obtained as white solid (5.1 mg, 27% yield). The analytical HPLC trace of the purified product is reported as Supporting Information. HRMS (ESI): $[M+Na]^+$ *m/z* calcd., 1020.3333; found, 1020.3328.

***N*^{3}-((3S,7S,11S)-7,11-Bis(2,3-dihydroxybenzamido)-2,6,10-trioxo-1,5,9-trioxacyclododecan-3-yl)-4,5-dihydroxy-*N*^{1}-(1-(naphthalen-2-yl)-1-oxo-5,8,11-trioxa-2-azatridecan-13-yl)isophthalamide (32).** Compound **32** was synthesized as described for **29** except that **15** (20 mg, 44 ⌠mol) was used instead of **7**. After purification by preparative TLC (5% MeOH/CH_2Cl_2), the benzyl-protected precursor of **32** was obtained as a white-yellow oily solid (37 mg, 59%). TLC R_f = 0.6 (10% MeOH/CH_2Cl_2). ^{1}H NMR ($CDCl_3$, 500 MHz), δ 3.44-3.74 (16H, m), 3.94-4.08 (4H, m), 4.12-4.16 (2H, m), 4.78-4.82 (1H, m), 4.87-4.92 (2H, m), 5.02-5.17 (12H, m), 7.01-7.52 (39H, m), 7.58-7.59 (1H, m), 7.64-7.66 (2H, m), 7.79-7.84 (3H, m), 7.94-7.94 (1H, m), 8.29-8.31 (1H, m), 8.47-8.50 (3H, m). ^{13}C NMR ($CDCl_3$, 125 MHz), δ 39.6, 39.9, 51.4, 51.4, 63.9, 64.1, 69.6, 69.7, 70.2, 70.4, 71.1, 71.2, 71.2, 76.2, 76.3, 76.3, 116.7, 117.5, 120.3, 123.1, 124.3, 124.6, 125.0, 125.2, 125.4, 126.1, 126.2, 126.2, 126.9, 127.6, 127.6, 127.9, 128.1, 128.2, 128.4, 128.4, 128.5, 128.6, 128.6, 128.8, 128.9, 128.9, 129.0, 130.0, 130.1, 130.3, 133.5, 134.5, 135.4, 135.7, 135.9, 136.0, 136.2, 146.9, 146.9, 149.0, 151.6, 151.7, 164.2, 164.9, 164.9, 165.7, 168.9, 169.0, 169.1, 169.6. HRMS (ESI): $[M+Na]^+$ *m/z* calcd., 1604.5837; found, 1604.5964. Compound **32** was purified by semi-preparative HPLC (20% B for 5 min followed by 30-55% B over 10 min, 4 mL/min) and eluted at 12.7 min. The isolated product was lyophilized and obtained as a white solid (4.4 mg, 18%). The analytical HPLC trace of the purified product is provided as Supporting Information. HRMS (ESI): $[M+Na]^+$ *m/z* calcd., 1064.3020; found, 1064.3084. Mass spectrometric analysis of the crude reaction indicated M+4 in addition to the

desired product **32** and suggested partial reduction of the naphthalene cargo under the deprotection conditions. From analysis of HPLC peak areas, the ratio between **32** and the partial reduction product is ca. 4:1.

***N*^{1}-(1-(3-Benzylphenyl)-1-oxo-5,8,11-trioxa-2-azatridecan-13-yl)-*N*^{3}-((3S,7S,11S)-7,11-bis(2,3-dihydroxybenzamido)-2,6,10-trioxo-1,5,9-trioxacyclododecan-3-yl)-4,5-dihydroxyisophthalamide (33).** Compound **33** was synthesized as described for **29** except that **16** (24 mg, 62 μmol) was used instead of **7**. Partial purification by preparative TLC (10% MeOH/CH_2Cl_2) afforded the benzyl-protected precursor of **33** as a white-yellow solid with a grease contamination (43 mg, 67%). TLC R_f = 0.6 (10% MeOH/CH_2Cl_2). ^{1}H NMR ($CDCl_3$, 500 MHz), δ 3.57-3.61 (12H, m), 3.94-3.95 (2H, d, *J* = 6.0) 3.97-4.05 (3H, m), 4.07-4.15 (3H, m), 4.85-4.90 (3H, m), 5.01-5.17 (12H, m), 7.01-7.40 (30H, m) 7.62-7.70 (3H, m), 7.82 (1H, d, J=2.0), 7.99-8.00 (1H, d, *J* = 2.0), 8.47-8.51 (3H, m) HRMS (ESI): $[M+Na]^+$ *m/z* calcd., 1644.6150; found, 1644.6105. A portion (32.5 mg, 20.0 μmol) of this material was carried on without further purification or characterization. Compound **33** was purified by semi-preparative HPLC (20% B for 5 min followed by 20-70% B over 15 min, 4 mL/min). The product eluted at 15.8 min and was obtained as white solid (13.5 mg, 62%). The analytical HPLC trace of the purified product is provided as Supporting Information. HRMS (ESI): $[M+Na]^+$ *m/z* calcd., 1104.3333; found, 1104.3305.

***N*^{3}-((3S,7S,11S)-7,11-Bis(2,3-dihydroxybenzamido)-2,6,10-trioxo-1,5,9-trioxacyclododecan-3-yl)-4,5-dihydroxy-*N*^{1}-(1-oxo-1-(11-oxo-2,3,5,6,7,11-hexahydro-1*H*-pyrano[2,3-*f*]pyrido[3,2,1-*ij*]quinolin-10-yl)-5,8,11-trioxa-2-azatridecan-13-yl)isophthalamide (34).**Compound **34** was synthesized as described for **29** except that **17** (18 mg, 39 μmol) was used instead of **7**. After purification by preparative TLC (10% MeOH/CH_2Cl_2) the benzyl-protected precursor of **34** was obtained as an orange oily solid (18 mg, 26%). TLC R_f = 0.7 (10% MeOH/CH_2Cl_2). ^{1}H NMR ($CDCl_3$, 500 MHz), δ 1.93-1.95 (4H, m), 2.71-2.83 (4H, m), 3.26-3.32 (4H, m), 3.56-3.69 (16H, m), 3.99-4.18 (6H, m), 4.88-4.94 (3H, m), 5.01-5.18 (12H, m), 6.94 (1H, s), 7.06-7.43 (35H, m), 7.62-7.66 (2H, m), 7.80-7.80 (1H, m), 7.97-7.97 (1H, m),

8.47-8.53 (4H, m), 9.02-9.03 (1H, m). ^{13}C NMR ($CDCl_3$, 125 MHz), δ 19.9, 20.0, 21.0, 27.3, 39.4, 40.1, 49.7, 50.2, 51.5, 64.1, 69.9, 71.1, 71.2, 76.3, 105.4, 108.1, 115.9, 117.5, 119.8, 123.0, 124.3, 125.7, 126.3, 127.2, 127.6, 127.6, 127.8, 128.1, 128.2, 128.5, 128.5, 128.6, 128.9, 128.9, 129.0, 130.0, 135.7, 136.0, 136.2, 146.9, 148.2, 148.3, 149.0, 151.6, 151.7, 152.6, 162.9, 164.4, 165.0, 165.0, 168.9, 169.1. HRMS (ESI): $[M+Na]^+$ *m/z* calcd.,1717.6313; found, 1717.6287. Compound **34** was purified by semi-preparative HPLC (20% B for 5 min followed by 20-70% B over 15 min, 4 mL/min). The product eluted at 17.1 min and was obtained as an orange solid (4.5 mg, 48%). The analytical HPLC trace of the purified product is provided as Supporting Information. HRMS (ESI): $[M+Na]^+$ *m/z* calcd., 1177.3496; found, 1177.3540.

7-(4-(1-(3-(((3S,7S,11S)-7,11-Bis(2,3-dihydroxybenzamido)-2,6,10-trioxo-1,5,9-trioxacyclododecan-3-yl)carbamoyl)-4,5-dihydroxyphenyl)-1-oxo-5,8,11-trioxa-2-azatetradecan-14-oyl)piperazin-1-yl)-1-cyclopropyl-6-fluoro-4-oxo-1,4-dihydroquinoline-3-carboxylic acid (35). Compound **35** was synthesized as described for **29** except that **18** (26 mg, 48 ∫mol) was used instead of 7, and TMSCl (10 ∫L, 79 ∫mol) and DIPEA (15 µL, 160 µmol) was mixed with **18** before addition to the solution containing **25**. After purification by preparative TLC (10% MeOH/CH_2Cl_2), the benzyl-protected precursor of **35** was obtained as a yellow oily solid (46 mg, 65%). TLC R_f = 0.65 (10% MeOH/CH_2Cl_2). ^{1}H NMR ($CDCl_3$, 500 MHz), δ 1.13 (2H, bs), 1.33 (2H, bs), 2.64 (2H, bs), 3.23-3.30 (4H, m), 3.51 (1H, bs), 3.63 (14H, bs), 3.79 (4H, bs), 3.99-4.04 (3H, m), 4.11-4.14 (3H, m), 4.86-4.91 (3H, m), 5.01-5.19 (12H, m), 7.06-7.43 (39H, m), 7.59-7.61 (2H, m), 7.83 (1H, s), 7.97-7.99 (2H, m), 8.45-8.49 (3H, m), 8.69 (1H, s). ^{13}C NMR ($CDCl_3$, 125 MHz), δ 8.2, 33.4, 35.4, 40.0, 41.1, 45.3, 49.3, 50.0, 51.3, 51.4, 51.4, 63.9, 64.1, 67.1, 69.7, 70.2, 70.3, 70.4, 70.5, 71.2, 71.3, 76.2, 76.3, 105.2, 108.0, 112.3, 112.4, 116.7, 117.5, 120.0, 120.0, 120.5, 123.0, 124.3, 125.6, 126.1, 126.1, 127.6, 127.6, 127.8, 128.2, 128.3, 128.4, 128.4, 128.5, 128.6, 128.6, 128.8, 128.8, 128.8, 129.0, 130.2, 135.5, 135.7, 135.9, 136.0, 136.1, 138.9, 145.2, 145.3, 146.8, 146.8, 147.4, 149.0, 151.6, 151.6, 151.8, 152.4, 154.4, 164.2, 164.9, 164.9, 165.8, 166.9, 168.9, 169.0, 169.1, 169.7, 176.9. ^{19}F NMR ($CDCl_3$, 282 MHz) *δ* -121.3. HRMS (ESI): $[M+Na]^+$ *m/z* calcd., 1792.6434; found, 1792.6337. Compound **35** was

purified by semi-preparative HPLC (20% B for 5 min followed by 20-70% B over 10 min, 4 mL/min) and eluted at 15.2 min. The isolated product was lyophilized and obtained as a white solid (2.5 mg, 9%). The HPLC trace of the purified product is provided as Supporting Information. HRMS (ESI): $[M+Na]^+$ *m/z* calcd., 1252.3617; found, 1252.3633.

7-(4-(6-Aminohexanoyl)piperazin-1-yl)-1-cyclopropyl-6-fluoro-4-oxo-1,4-dihydro-quinoline-3-carboxylic acid (36). Ciprofloxacin (**37**, 331 mg, 1.00 mmol) and DIPEA (1.0 mL, 5.7 mmol) were mixed in 6 mL of dry CH_2Cl_2, and TMSCl (370 μL , 2.91 mmol) was added to give a clear yellow solution. 6-((Tert-butoxycarbonyl)amino)hexanoic acid (**12**, 346 mg, 1.50 mmol), PyAOP (834 mg, 1.60 mmol), and DIPEA (700 μL, 4.02 mmol) were dissolved in 4 mL of dry CH_2Cl_2, and the two solutions were combined and stirred overnight at rt. The reaction was quenched with MeOH (10 mL), and the resulting solution was concentrated to dryness, and the crude product was redissolved in 40 mL of EtOAc. The organic phase was washed with 10 mM HCl (2 x 40 mL) and saturated aqueous $NaHCO_3$ (2 x 40 mL), dried over Na_2SO_4, and purified by flash chromatography on silica gel (3% MeOH/CH_2Cl_2) to give **38** as yellow solid (243 mg, 45%). TLC R_f = 0.7 (5% MeOH/CH_2Cl_2). ^{1}H NMR ($CDCl_3$, 300 MHz), *δ* 1.14-1.20 (2H, m), 1.32-1.53 (13H, m), 1.59-1.69 (2H, m), 2.36 (2H, t, *J* = 6.0 Hz), 3.08 (2H, dt, *J* = 6.3, 6.3 Hz), 3.26-3.56 (4H, m), 3.51-3.59 (1H, m), 3.69-3.82 (4H, m), 4.68 (1H, bs), 7.32 (1H, d, *J* = 7.2 Hz), 7.82 (1H, d, *J* = 12.9 Hz), 8.60 (1H, s), 14.9 (1H, bs). ^{13}C NMR ($CDCl_3$, 125 MHz), δ 8.1, 24.7, 26.4, 28.3, 29.8, 32.9, 35.3, 40.2, 41.0, 45.1, 49.3, 49.9, 78.9, 105.0, 107.7, 111.9, 112.1, 119.6, 119.7, 138.8, 145.2, 145.3, 147.3, 152.4, 154.4, 155.9, 166.6, 171.4, 176.7. ^{19}F NMR ($CDCl_3$, 282 MHz), δ -121.1. HRMS (ESI): $[M+H]^+$ *m/z* calcd., 545.2775; found, 545.2768.

The TFA salt of **36** (202 mg, 98%) was obtained as a yellow solid from **38** (201 mg, 0.369 mmol) by stirring **38** in 40% TFA/CH_2Cl_2 at rt for 3 h and removing the solvent. TLC R_f = 0.1 (10% MeOH/CH_2Cl_2). ^{1}H NMR (CD_3OD, 300 MHz), δ 1.41-1.52 (4H, m), 1.65-1.77 (4H, m), 2.52 (2H, t, *J* = 7.2 Hz), 2.96 (2H, t, *J* = 7.2 Hz), 3.34-3.43 (4H, m), 3.82 (5H, m), 7.57 (1H, d, *J* = 7.5 Hz), 7.85 (1H, d, *J* = 13.2 Hz), 8.76 (1H, s). ^{13}C NMR ($CDCl_3$, 125 MHz), δ 7.8, 23.8, 25.4, 26.5, 26.6, 32.2, 35.4, 39.0, 39.1, 41.0, 45.0, 48.1, 48.3, 48.5, 48.6, 48.8, 49.0, 49.1, 49.5, 105.0,

107.0, 111.6, 111.8, 119.3, 119.4, 138.8, 145.1, 145.2, 147.4, 152.3, 154.3, 167.3, 171.8, 176.5. ^{19}F NMR ($CDCl_3$, 282 MHz), δ -76.0, -120.9. HRMS (ESI): $[M+H]^+$ *m/z* calcd., 445.2251; found, 445.2255.

7-(4-(6-(3-(((3S,7S,11S)-7,11-Bis(2,3-dihydroxybenzamido)-2,6,10-trioxo-1,5,9-trioxacyclododecan-3-yl)carbamoyl)-4,5-dihydroxybenzamido)hexanoyl)piperazin-1-yl)-1-cyclopropyl-6-fluoro-4-oxo-1,4-dihydroquinoline-3-carboxylic acid (40). Compound **40** was synthesized as described for **35** except that DMSO (1.5 mL) was used as the solvent and compound **36** (19.4 mg, 34.8 ∫mol) was used instead of **18**. After preparative TLC purification (10% MeOH/CH_2Cl_2), **39** was obtained as white viscous solid (17 mg, 74%). TLC R_f = 0.6 (10% MeOH/CH_2Cl_2). ^1H NMR ($CDCl_3$, 300 MHz) δ 1.17-1.83 (10H, m), 2.40 (2H, bs), 3.29-3.44 (6H, m), 3.70-3.86 (5H, m), 4.02-4.17 (6H, m), 4.86-4.93 (3H, m), 5.04-5.21 (12H, m), 7.07-7.42 (33H, m), 7.60-7.64 (2H, m), 7.85-8.05 (3H, m), 8.47-8.50 (3H, m), 8.74 (1H, bs), 15.0 (1H, bs).^{13}C NMR ($CDCl_3$, 125 MHz), δ 8.1, 12.3, 17.2, 18.6, 24.4, 26.3, 26.4, 26.5, 29.0, 32.8, 34.7, 39.7, 41.2, 45.3, 46.2, 46.3, 51.4, 51.5, 51.5, 52.0, 54.8, 63.9, 64.1, 64.2, 71.1, 71.2, 71.2, 76.2, 76.3, 76.3, 105.2, 109.5, 113.0, 113.2, 116.6, 117.5, 120.1, 123.0, 124.3, 125.5, 126.1, 127.6, 127.8, 128.2, 128.3, 128.4, 128.4, 128.5, 128.6, 128.6, 128.6, 128.8, 128.9, 128.9, 129.0, 130.3, 135.5, 135.8, 135.9, 136.0, 136.1, 138.1, 145.4, 146.8, 148.4, 149.0, 151.6, 151.8, 152.3, 164.4, 164.9, 165.0, 165.8, 166.1, 168.8, 169.0, 169.1, 171.5. HRMS (ESI): $[M+H]^+$ *m/z* calcd., 1680.6303; found, 1680.6352. Compound **40** was purified by semi-preparative HPLC (20% B for 5 min followed by 20-70% B over 15 min, 4 mL/min) and eluted at 16.1 min. The isolated product was lyophilized and obtained as a white-yellow solid (6.7 mg, 59%). The HPLC trace of the purified product is provided as Supporting Information. HRMS (ESI): $[M+H]^+$ *m/z* calcd., 1140.3486; found, 1140.3482.

***N*$_1$-(2-(2-(2-(2-Azidoethoxy)ethoxy)ethoxy)ethyl)-4,5-bis(benzyloxy)-*N*$_3$-((3S,7S,11S)-7,11-bis(2,3-bis(benzyloxy)benzamido)-2,6,10-trioxo-1,5,9-trioxacyclododecan-3-yl)isophthalamide (41).** 11-Azido-3,6,9-trioxaundecan-1-amine (**11**, 8.2 ∫L, 42 ∫mol) and **25** (40 mg, 32 μmol) were dissolved in 1 mL of dry CH_2Cl_2. PyAOP (33.2 mg, 63.8 ∫mol) and

DIPEA (22.2 ⌠L, 128 ⌠mol) were added to give a light yellow solution. The reaction was stirred for 4 h at rt and concentrated, and the crude product was purified by preparative TLC (50% EtOAc/CH_2Cl_2) to afford **41** as a light yellow oil (31 mg, 68%). TLC R_f = 0.3 (50% EtOAc/CH_2Cl_2). ^{1}H NMR ($CDCl_3$, 300 MHz) δ 3.34 (2H, t, *J* = 5.1 Hz), 3.61-3.69 (14H, m), 3.97-4.18 (6H, m), 4.88-4.94 (3H, m), 5.02-5.22 (12H, m), 7.08-7.46 (34H, m), 7.64-7.67 (2H, m), 7.85 (1H, d, *J* = 1.8 Hz), 7.99 (1H, d, *J* = 2.1 Hz), 8.48-8.52 (3H, m). ^{13}C NMR ($CDCl_3$, 125 MHz) δ 40.0, 50.6, 51.4, 64.0, 64.1, 69.7, 69.9, 70.3, 70.6, 71.2, 71.2, 76.3, 116.7, 117.5, 120.4, 123.1, 124.3, 125.5, 126.2, 126.2, 127.6, 127.6, 127.9, 128.3, 128.4, 128.4, 128.5, 128.6, 128.7, 128.8, 128.9, 129.0, 130.2, 135.5, 135.8, 136.0, 136.0, 136.2, 146.9, 146.9, 149.1, 151.6, 151.8, 164.2, 164.9, 164.9, 165.9, 168.9, 169.1, 169.1. HRMS (ESI): $[M+Na]^+$ *m/z* calcd., 1476.5323; found, 1476.5345.

Vancomycin-PEG-Ent (42). A DMSO solution of **41** (19 mg/mL, 1.3 mM, 250 µL), an aqueous solution of **8** (20 mg/mL, 1.3 mM, 250 µL), a DMF solution of benzoic acid (49 mg/mL, 450 mM, 50 µL), and an aqueous solution of $CuSO_4$ (10 mg/mL, 45 mM, 50 µL) were mixed together, and an additional 400 µL of DMSO was added to yield a clear light blue solution. An aqueous solution of sodium ascorbate (NaAsc, 18 mg/mL, 90 mM, 50 µL) was subsequently added. The reaction become colorless to yellow and was stirred at rt for 15 min, at which time another 50 µL of aqueous NaAsc was added. After stirring for 15 min, the crude reaction was frozen and lyophilized to give a brown oil. The oil was dissolved in a 2:1:1 ratio of dioxane/MeOH/H_2O and purified by semi-preparative HPLC (50% B for 5 min followed by 50-100% B over 11 min, 4 mL/min). The benzyl-protected precursor of **42** eluted at 13 min and was obtained as white solid after lyophilization (3.5 mg, 36%). HRMS (ESI): $[M+2Na]^{2+}/2$ *m/z* calcd., 1520.5030; found, 1520.5171.

A portion of this precursor (14 mg, 4.7 ⌠mol; obtained from four 250-µL scale Click reactions) was dissolved in 30% H_2O/MeOH, the flask was purged with N_2, and 16 mg Pd/C (10% wt) was added. The reaction was stirred under H_2 (1 atm) for 24 h at rt, and the Pd/C was removed by centrifugation (13,000 rpm, 10 min). The supernatant was concentrated by

lyophilization and the resulting residue was dissolved in a 2:1:1 mixture of dioxane/MeOH/H_2O. HPLC purification (20% B for 5 min followed by 20-46% B over 8 min, 4 mL/min) gave **43** as white solid (6.3 mg, 55%). The HPLC trace of the purified product is reported in Supporting Information. HRMS (ESI): $[M+2H]^{2+}/2$ *m/z* calcd., 1228.37960; found, 1228.37961.

***tert*-Butyl(2-(((1-(1-(3-(((3S,7S,11S)-7,11-bis(2,3-dihydroxybenzamido)-2,6,10-trioxo-1,5,9-trioxacyclododecan-3-yl)carbamoyl)-4,5-dihydroxyphenyl)-1-oxo-5,8,11-trioxa-2-azatridecan-13-yl)-1H-1,2,3-triazol-4-yl)methyl)amino)-2-oxoethyl)carbamate (43).** Compound **43** was synthesized as described for **42** except that a DMSO solution of **7** (2.8 mg/mL, 13 mM, 25 μL) was used instead of **8**. HPLC purification gave 3.3 mg of the benzyl-protected precursor of **43** as a white solid (58%). HRMS (ESI): $[M+H]^+$ *m/z* calcd., 1688.6489; found, 1688.6421. Compound **43** (3.3 mg, 33%) was obtained from the precursor (13.3 mg, 7.88 μmol; obtained from four 25-μL scale Click reactions) following the same procedure as synthesizing **42**. HPLC purification (0% B for 5 min followed by 0-45% B over 8 min, 4 mL/min) afforded **43** as a white solid with a retention time of 12.8 min. The HPLC trace of the purified product is reported as Supporting Information. HRMS (ESI): $[M+H]^+$ *m/z* calcd., 1126.3853; found, 1126.3832.

Growth Recovery Assays. General microbiology methods are included as Supporting Information. Overnight cultures were prepared by inoculating 5 mL of LB (*E. coli*) or LB base supplemented with 2.5 g/L NaCl (*P. aeruginosa*) with the appropriate freezer stocks and the cultures were incubated at 37 ^oC in a tabletop incubator shaker set at 150 rpm. The overnight culture was diluted 1:100 into 5 mL of fresh media with or without 200 μM 2,2'-dipyridyl (DP) and incubated at 37 ^oC with shaking at 150 rpm until the optical density at 600 nm (OD_{600}) reached 0.6. The cultures were diluted to an OD_{600} value of 0.001 in 50% reduced MHB medium (10.5 g/L) with or without 200 μM (*E. coli*) or 600 μM DP (*P. aeruginosa*). A 90-μL aliquot of the diluted culture was mixed with a 10-μL aliquot of a 10x solution of the siderophore or siderophore-cargo conjugate in a 96-well plate, which was wrapped in parafilm and incubated at 30 °C with shaking at 150 rpm for 19 h. Bacterial growth was assayed by measuring OD_{600}

using a BioTek Synergy HT plate reader. Each well condition was prepared in duplicate and three independent replicates of each assay were conducted on different days. The resulting mean OD_{600} are reported and the error bars are the standard deviation of the mean obtained from the three independent replicates.

Results and Discussion

Design and Synthesis of Monofunctionalized Enterobactin Platforms. We present a stepwise synthesis to monofunctionalized enterobactin scaffolds in Scheme 1. Guided by the structures of MGE and DGE (Figure 1A), we chose to install functional groups amenable to synthetic modification at the C5 position of one enterobactin catechol ring. This position is remote from the iron-binding hydroxyl groups in addition to the macrolactone (Figure 2). Prior studies of the salmochelins indicate that modification at this site compromises neither Fe(III) complexation nor the esterase-catalyzed hydrolysis of the macrolactone.[33,64] The structure of the antibiotic-siderophore conjugate MccE492m (Figure S1),[65] which exhibits a monoglucosylated enterobactin derivative attached to a ribosomal peptide, also influenced our decision to prepare monofunctionalized enterobactin platforms. We selected methyl-5-allyl-3-methoxysalicylate **19** as a starting material because of its commercial availability. This precursor was demethylated using BBr_3 in the presence of DIPEA to prevent HBr addition to the alkene moiety, and **20** was obtained in 53% yield as a white powder. Benzyl protection of **20** and subsequent hydrolysis of the methyl ester in refluxing sodium hydroxide was performed following a literature protocol[62] for catecholate protection of 2,3-dihydroxybenzoic acid and **21** was obtained in 99% yield as a white powder. Palladium-catalyzed isomerization of the alkene was achieved by using $PdCl_2$ in degassed methanol and **22** was obtained in 89% yield as a light yellow solid following workup. Next, a one-pot coupling reaction between the enterobactin trilactone **4**, **6** and **22** was performed with a 1:1.5:1 ratio and PyAOP as the coupling reagent. This reaction provided a mixture of **23**, its di- and tri-substituted analogs, and unmodified Ent. These products were separated by flash chromatography and afforded **23** in 37% yield as a

white foam. The 1:1.5:1 ratio of **4**/**6**/**22** was chosen based on several optimization trails and this ratio provided the highest yield of the desired monosubstituted product. Oxidation of alkene **23** by using OsO_4 and $NaIO_4$ in mixed 1,4-dioxane/water afforded **24** as a white foam in 58% yield. Further oxidation of **24** under mild conditions provided carboxylic acid **25** in 76% yield as a white powder. This step-wise synthesis provides gram quantities of **23-25** (L-isomers) in high purity, and these molecules are stable when stored as dry solids at 4 ^{o}C. The stepwise coupling and oxidations were also performed using triserine lactone **5** to afford the D-enantiomers alkene **26**, aldehyde **27**, and acid **28** (Supporting Information). The D-enantiomer of Ent is transported into *E. coli* by FepA, but it is not a substrate for the enterbactin esterase Fes.[66] We therefore reasoned that conjugates based on D-Ent would provide useful controls for conjugate uptake studies, and that this enantiomer may also be advantageous in antibacterial drug delivery applications because it provides an iron-starvation effect.

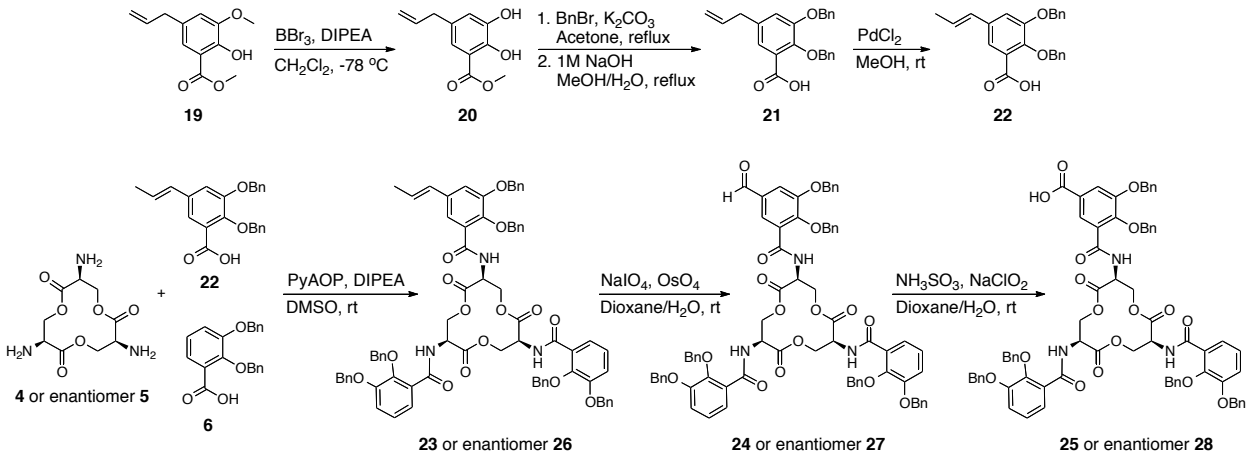

Scheme 1. Syntheses of **22** (top) and monofunctionalized enterobactin scaffolds (bottom).

This synthesis provides a family of enterobactin scaffolds amenable to functionalization. For instance, alkene **23** may be employed in olefin cross metathesis,[67] aldehyde **24** in reductive amination, and acid **25** in peptide coupling reactions. Moreover, other organic transformations of

22 or **23** may provide additional versatile functional groups (e.g. hydroxyl), affording more synthetic possibilities for enterobactin derivatives that can be utilized in various applications.

Design and Synthesis of Enterobactin-Cargo Conjugates. We selected carboxylic acid **25** as a key intermediate for the preparation of enterobactin-cargo conjugates, and evaluated two strategies for appending cargo to the enterobactin scaffold. In one thrust, standard peptide coupling chemistry was employed to link cargo to the enterobactin acid via an amide bond (Schemes 2 and 3). In the second approach, enterobactin-azide **41** was prepared and "Click" chemistry utilized for cargo attachment (Scheme 4). In both cases, benzyl deprotection unmasked the enterobactin catecholates in the final step.

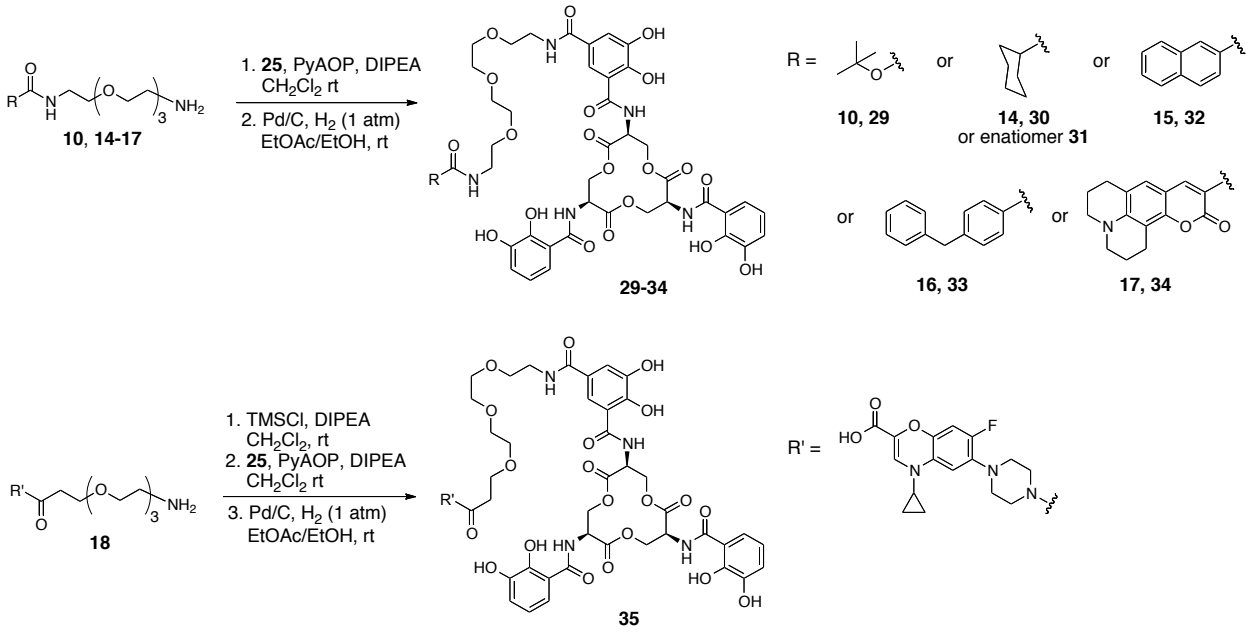

Scheme 2. Syntheses of enterobactin-cargo conjugates **29**-**35**. The syntheses of **14**-**18** are provided as Supporting Information.

We selected a variety of commercially available molecules housing carboxylic acids as cargos. The cargos presented in Scheme 2 vary in size and shape and include a simple Boc

protecting group, cyclohexane, naphthalene, phenylmethylbenzene, ciprofloxacin, and coumarin 343. This selection includes cargo expected to be non-toxic (e.g. Boc, cyclohexane) in addition to an antibiotic (ciprofloxacin) and a fluorophore (coumarin 343). Next, we selected PEG_3 as a stable and water-compatible linker. It provides ca. 14-Å separation between enterobactin and the cargo. The conjugates depicted in Scheme 2 were prepared by coupling the PEG-derivatized cargo **10,14-18** to **25** using PyAOP as the coupling reagent. The resulting benzyl-protected conjugates were purified by preparative TLC and obtained in yields ranging from 26% (Bn-**34**) to 75% (Bn-**29**). Benzyl deprotection reactions were performed by hydrogenation over Pd/C and the resulting enterobactin-cargo conjugates were purified by reverse-phase semi-preparative HPLC. Conjugates **29-35** were obtained in milligram quantities and high purity judging by analytical HPLC (Figures S2-S11) and LC/MS analysis (Table S1). Conjugate **31** houses D-Ent and was prepared to probe the role of Fes-mediated hydrolysis in the bacterial growth recovery assays (*vide infra*).

Scheme 3 exhibits the synthesis of enterobactin-ciprofloxacin **40** where the PEG linker is substituted by a C_5 alkyl chain to probe the consequences of variable linker composition and hydrophilicity. The synthesis of **40** was carried out by reacting ciprofloxacin with 6-Boc-aminohexanoic acid **12** followed by Boc deprotection, coupling of the resulting free amine to **25**, and benzyl deprotection. The carboxylic acid of ciprofloxacin was protected *in situ* by using trimethylsilyl chloride (TMSCl) to prevent self-coupling in the syntheses of both **35** and **40**. In this general approach of attaching a carboxylic acid cargo, the linkers were first coupled to the cargo rather than to the Ent scaffold because the Ent macrolactone degrades in the presence of primary amines and under highly acidic conditions such as those required to remove Boc protecting groups.

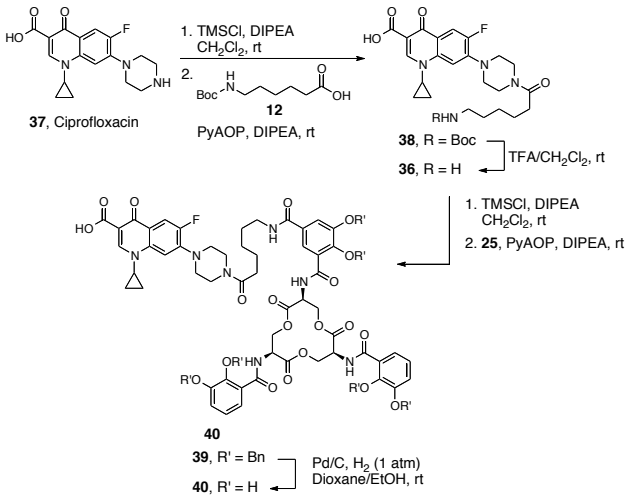

Scheme 3. Synthesis of enterobactin-ciprofloxacin conjugate **40**.

In Scheme 4, we present the synthesis of **43**, an enterobactin-vancomycin conjugate assembled via Click chemistry. Vancomycin is a nonribosomal peptide antibiotic active against Gram-positive organisms that inhibits cell wall biosynthesis by binding to the D-Ala-D-Ala of lipid II and blocking peptidoglycan cross-linking.[68] It exhibits poor activity against Gram-negative bacteria because it is too large to cross the outer membrane. Because modification of the C-terminal carboxylic acid with a PEG chain did not perturb its antibacterial activity,[69] we selected this site as a point of attachment. Moreover, we employed Click chemistry for the conjugate assembly to avoid complications with the various functional groups exhibited by vancomycin. First, the azide-functionalized PEG linker **11** was coupled to **25** to afford the enterobactin-azide **41** in 68% yield. Copper(I)-catalyzed azide-alkyne cycloaddition of **41** with alkyne **8**[63] subsequently afforded enterobactin-vancomycin **42** in 55% yield following hydrogenation and purification. This synthetic approach was extended to **43**, a small analog of **42** that houses a *tert*-butyl cargo, and the strategy is also applicable to other alkyne-substituted cargos that are compatible with the benzyl deprotection conditions.

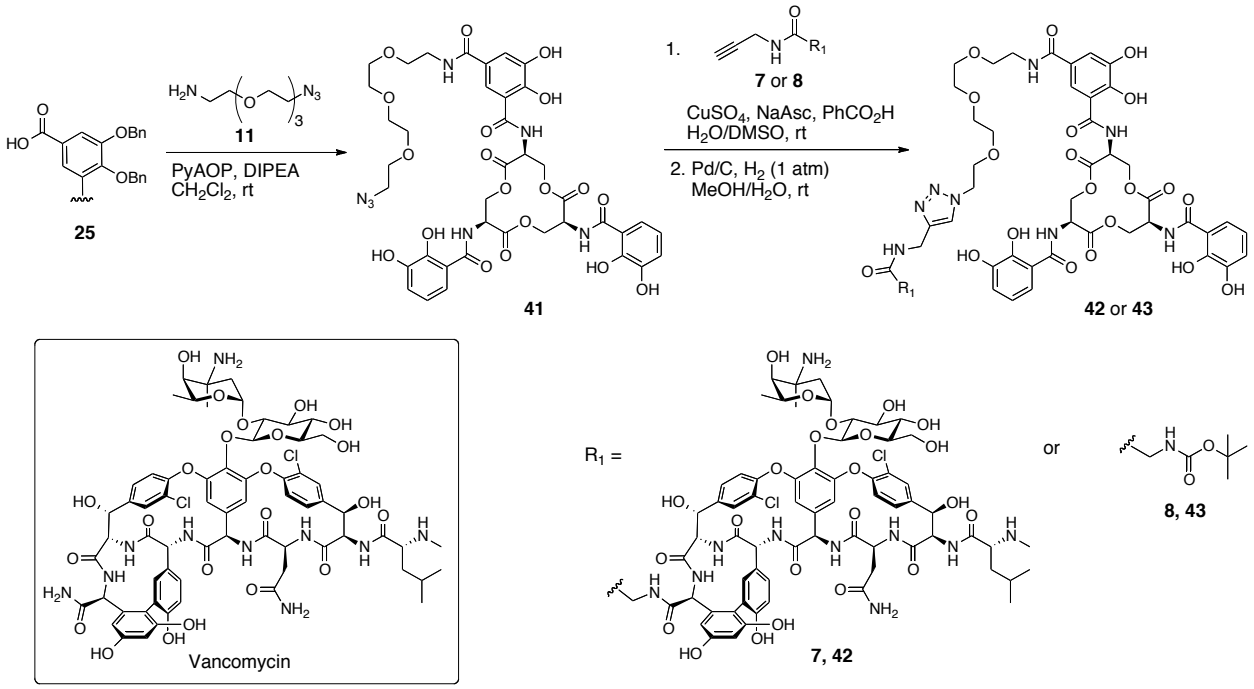

Scheme 4. Syntheses of enterobactin-cargo conjugates by Click chemistry.

Enterobactin-Cargo Conjugates Coordinate Fe(III). The optical absorption spectrum of each enterobactin-cargo conjugate exhibited catecholate absorption at ca. 316 nm (MeOH, rt). With the exception of **34**, which afforded a yellow solution because of the coumarin moiety, methanolic solutions of each conjugate turned from colorless to wine-colored following the addition of ca. one equiv of aqueous Fe(III), and the expected ligand-to-metal charge transfer (LMCT) bands were observed, indicating Fe(III) coordination to the enterobactin catecholates (Figure S12-S14).[70]

Enterobactin-Cargo Conjugate Delivery to the *E. coli* Cytoplasm. We employed three non-pathogenic *E. coli* strains that are defective in enterobactin synthesis, enterobactin transport, or ferric enterobactin utilization in growth recovery assays (Table S2). *E. coli* ATCC 33475 (*ent*-) cannot biosynthesize enterobactin, but retains the capacity to import and metabolize the siderophore.[71] *E. coli* H1187 (*fepA-)* lacks the outer membrane enterobactin

receptor. *E. coli* K-12 JW0576 (*fes*-) can accumulate ferric enterobactin, but cannot release the iron because it is deficient in the enterobactin esterase Fes. As a result of these defects in iron metabolism, all three strains grow poorly under conditions of iron limitation.[71] The iron chelator dipyridyl (DP) was used to generate iron-deficient conditions and promote expression of siderophore transport machinery in the growth recovery assays.

We first evaluated whether the enterobactin conjugates afforded growth recovery of *E. coli* (*ent*-) cultured under iron-deficient conditions (50% MHB, 200 μM DP). *E. coli* (*ent*-) grew to OD_{600} ~ 0.35 in 50% MHB medium (30 ^{o}C, t = 19 h), and this value decreased to <0.05 when 200 μM DP was added to the media. Low-micromolar concentrations of L-Ent restored growth, as expected,[70] and the *E. coli* cultures reached OD_{600} ~ 0.2 in the presence of 10 μM Ent (Figure 3). Likewise, low-micromolar concentrations of the enterobactin-cargo conjugates **29-33** and **43** exhibiting Boc (**29, 43**), cyclohexyl (**30**), napthyl (**32**), and phenylmethylbenzyl (**33**) cargos afforded growth recovery to similar levels (Figures 3 and S15). No growth restoration was observed when *E. coli* (*fepA*-) or *E. coli* (*fes*-) were cultured with **29** or **30** (Figures 5 and S16), which supports the notion that the growth recovery of *E. coli* (*ent*-) results from FepA-mediated cytoplasmic transport and Fes-catalyzed hydrolysis of the enterobactin moiety to release iron. Moreover, the D-enantiomer of enterobactin, D-Ent **9**, is not a substrate for Fes and does not provide growth recovery (Figures 4 and S17).[66] Indeed, no growth promotion occurred when *E. coli* (*ent*-) was treated with conjugate **31***,* the D-enantiomer of **30** (Figures 4 and S15). Taken together, these results demonstrate that the enterobactin transport machinery has the capacity to recognize and transport cargo-derivatized enterobactin scaffolds to the *E. coli* cytoplasm, and that these molecules are substrates for the cytoplasmic esterase Fes.

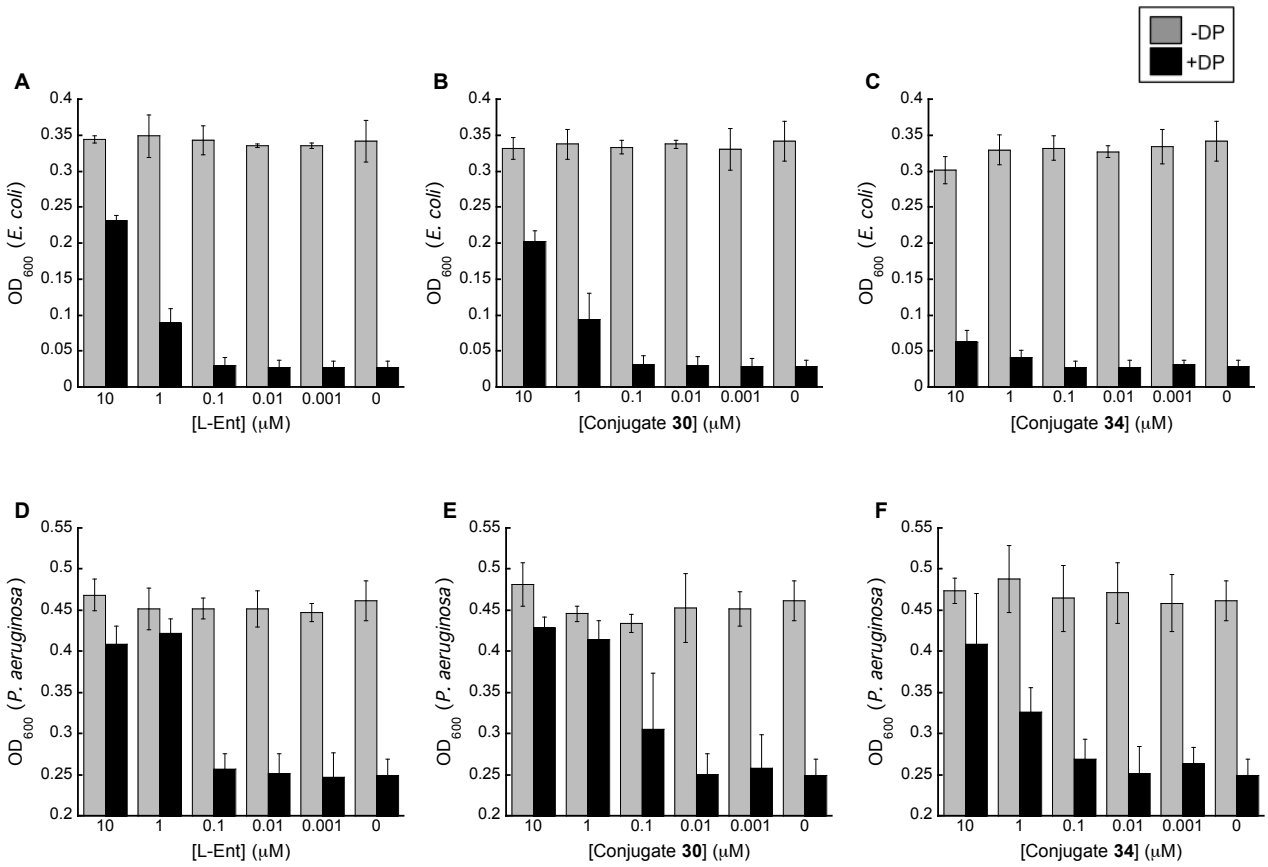

Figure 3. *E. coli* ATCC 33475 (*ent*-) and *P. aeruginosa* PAO1 (*pvd*-, *pch*-) growth recovery assays employing L-Ent and select enterobactin-cargo conjugates (50% MHB, ± 200 or 600 μM DP, t = 19 h, 30 °C). Grey bars: OD_{600} of bacteria cultured in the absence of DP. Black bars: OD_{600} of bacteria cultured in the presence of 200 (*E. coli*) or 600 (*P. aeruginosa*) μM DP. (A) L-Ent promotes growth recovery of *E. coli*. (B) Enterobactin conjugate **30** housing a cyclohexyl cargo affords growth recovery of *E. coli*. (C) Enterobactin conjugate **34** housing a coumarin moiety affords little-to-no growth recovery of *E. coli*. (D) L-Ent promotes growth recovery of *P. aeruginosa.* (E) Enterobactin conjugate **30** housing a cyclohexyl cargo affords growth recovery of *P. aeruginosa.* (F) Enterobactin conjugate **34** housing a coumarin moiety affords growth recovery of *P. aeruginosa*. Figures 4 and S15 contain the assay results for the other conjugates. Each bar indicates the average of three independent replicates (two wells per replicate) and the error bars are the standard deviation of the mean.

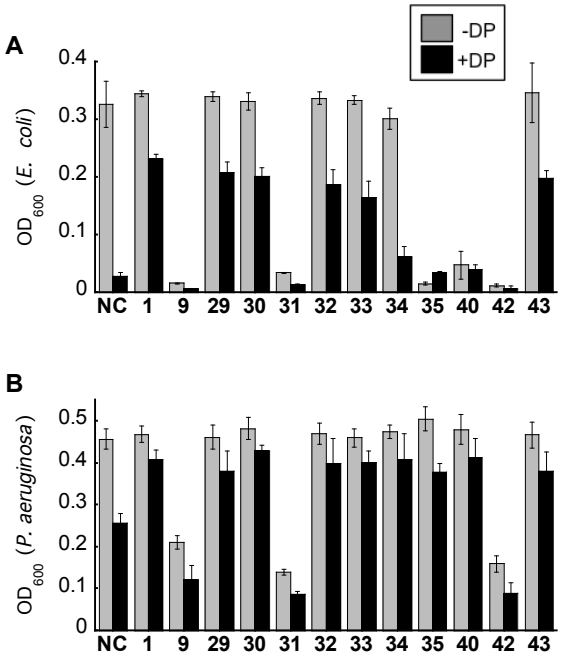

Figure 4. The comparative effects of enterobactin-cargo conjugates on bacterial cell growth. *E. coli* and *P. aeruginosa* were cultured in the presence of 10 μM of L-Ent **1**, D-Ent **9** and the enterobactin-cargo conjugates **29-35, 40, 42, 43** in the absence (grey bars) and presence (black bars) of DP (50% MHB, T = 30 °C, t = 19 h). (A) *E. coli* ATCC 33475 (*ent*-) and the DP concentration was 200 μM. (B) *P. aeruginosa* PAO1 (*pvd*-, *pch*-) and the DP concentration was 600 μM. NC refers to a no-conjugate control.

We observed no convincing evidence for marked uptake of larger cargos by *E. coli* ATCC 33475, which suggests that FepA of this *E. coli* strain has a cargo size limit. For instance, under iron limitation, negligible *E. coli* growth recovery and no toxicity was observed following treatment with the enterobactin-coumarin conjugate **34** (Figure 3), suggesting that *E. coli* (*ent*-) may not readily import **34**. Moreover, no growth recovery occurred following treatment of *E. coli* with either ciprofloxacin **35** or **40** (Figures 4 and S15). In the absence of DP, these conjugates afforded a concentration-dependent inhibition of *E. coli* growth. Likewise, 10 μM vancomycin **42**

inhibited the growth of *E. coli* (± DP, Figures 4 and S15). This behavior contrasts that of unmodified vancomycin, which is inactive against *E. coli* over the concentration range employed in this study. Two possible origins for inhibitory activity of the ciprofloxacin and vancomycin conjugates are (i) enterobactin-antibiotic uptake and resulting antibacterial action or (ii) a lack of active transport into *E. coli*, resulting in extracellular iron chelation and hence nutrient deprivation. Taking all observations into account, including those for *P. aeruginosa* described below, we contend that the latter option is the most probable explanation.

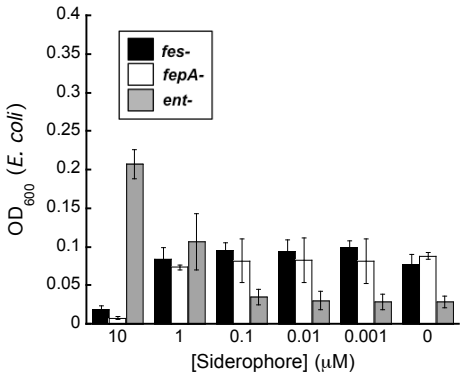

Figure 5. Comparison of growth recovery for *E. coli* (*ent-), E. coli* (*fepA*-), *and E. coli* (*fes*-) with conjugate **29** in the presence of 200 μM DP. Black bars: *E. coli* (*fes*-) cultured with conjugate **29**; white bars: *E. coli* (*fepA*-) cultured with conjugate **29** ; grey bars, *E. coli* (*ent*-) cultured with conjugate **29** in the presence of 200 μM DP. See Figures 4 and S16 for additional data.

Enterobactin-Cargo Conjugate Delivery to the *P. aeruginosa* Cytoplasm. We next sought to determine whether the enterobactin-cargo conjugates provided growth recovery for *Pseudomonas aeruginosa* PAO1. This Gram-negative opportunistic human pathogen synthesizes and exports two siderophores, pyoverdine (pvd) and pyochelin (pch), and employs

multiple additional mechanisms for iron acquisition.[72,73] *P. aeruginosa* utilizes enterobactin as a xenosiderophore, and the genes *pfeA*[74,75] and *pirA*[76] encode outer membrane enterobactin transporters. Similar to the *E. coli* experiments, we focused on using *P. aeruginosa* strains deficient in siderophore production or utilization in growth recovery assays. *P. aeruginosa* K648 (*pvd*-, *pch*-) is deficient in both pyoverdine and pyochelin biosynthesis, and shows attenuated growth in iron-deficient conditions, whereas *P. aeruginosa* K407 (*pvd*-, *pFr*-) is deficient in pyoverdine biosythesis and lacks the enterobactin transporter PfeA.[74]

In 50% MHB medium, *P. aeruginosa* (*pvd*-, *pch*-) grew to OD_{600} ~ 0.45 (30 ^{o}C, t = 19 h) and this value diminished to ca. 0.25 in the presence of 600 μM DP. Supplementation of the iron-limiting growth medium with low-micromolar concentrations of L-Ent resulted in the restoration of *P. aeruginosa* growth to OD_{600} ~ 0.40 (Figure 3). Comparable growth recovery was observed for cultures treated with eight of the nine conjugates based on L-Ent (Figures 3, 4 and S18). Vancomycin **42**, which exhibits the largest cargo, afforded a growth inhibitory effect (±DP) as observed for *E. coli* (*ent*-). In contrast to its L-Ent analog **30**, conjugate **31** based on D-Ent was growth inhibitory as was D-Ent (Figures 4 and S18). This result demonstrates that *P. aeruginosa* also requires the L-isomer for iron utilization. Lastly, no growth enhancement of *P. aeruginosa* (*pFr*-) was observed in the presence of L-Ent or conjugate **30** (600 μM DP); instead, these siderophores caused growth inhibition at micromolar concentrations (Figure S19). These results demonstrate that PfeA is necessary for conjugate-mediated growth recovery, supporting its role as a transporter for the enterobactin conjugates. In total, these assays demonstrate that the enterobactin transport machinery of *P. aeruginosa*, and PfeA in particular, recognizes and delivers various cargo-modified enterobactin scaffolds to the cytoplasm.

Ciprofloxacin is a fluoroquinolone antibiotic that acts in the cytoplasm and inhibits DNA gyrase.[77] The fact that ciprofloxacin conjugates **35** and **40** each restored *P. aeruginosa* growth demonstrated that the cargo was successfully delivered to the cytoplasm of this microbe with negligible impact of the variable linker composition, and that conjugation of ciprofloxacin to enterobactin attenuated its antibacterial activity. This observation is in general agreement with

reports of pyoverdine-fluoroquinoline[78] and pyochelin-fluoroquinoline[79,80] conjugates where the antibiotic was covalently attached to the siderophore and point to the need for appropriate linker design for fluoroquinolone delivery and release after cellular entry.[81] These pyoverdine/pyochelin-antibiotic conjugates afforded no antipseudomonal activity or diminished activity relative to the unmodified drug, and the pyoverdine-fluoroquinolone antibiotic exhibited decreased *E. coli* gyrase inhibitory activity *in vitro*.[78]

A comparison of the enterobactin-cargo growth recovery profiles for *E. coli* and *P. aeruginosa* (Figures 4, S15, S18) reveals that these particular microbes have different capacities for internalizing enterobactin-cargo conjugates, and that cargo size is an important factor. Vancomycin has a rigid dome-like structure and a molecular weight of ca. 1.4 KDa, and the assays presented in this work suggest that this molecule is too big for enterobactin-mediated transport into *E. coli* or *P. aeruginosa*. In contrast, small and malleable cargos such as a Boc protecting group and cyclohexane afforded growth recovery comparable to that of L-Ent for both strains. A comparison of OD_{600} values for bacterial cultures treated with such conjugates (e.g. **29**, **30**, **32**, **34**) shows that growth recovery to levels comparable to that of L-Ent occurs at a conjugate concentration of 1 μM for *P. aeruginosa* whereas 10 μM is required for *E. coli*. *P. aeruginosa* responds to lower Ent concentrations than *E. coli*, which indicates a higher uptake efficiency. Coumarin 343 is an example of a cargo that exhibits no signs of toxicity over the concentration range tested and affords markedly different results on microbial growth promotion for these two species. A comparison of the ciprofloxacin conjugate data for *E. coli* and *P. aeruginosa* also suggests differential uptake. For both the ciprofloxacin and coumarin cargo, the growth recovery assays indicate that the enterobactin transport machinery of *P. aeruginosa* imports these cargos whereas the *E. coli* system does not. These observations suggest that species-selective targeting may be possible with strategic cargo choice even when a siderophore is utilized by multiple microbial species.

Summary and Perspectives

We have designed and prepared a family of monofunctionalized enterobactin derivatives, and utilized these scaffolds for the preparation of enterobactin-cargo conjugates bearing cargos of varying size and complexity. Growth recovery assays employing *E. coli* and *P. aeruginosa* revealed that the enterobactin uptake machineries of these Gram-negative species recognize and transport enterobactin-cargo conjugates to the Gram-negative cytoplasm. These studies are significant in several respects. First, the notion of using siderophores for antibiotic delivery across the Gram-negative outer membrane, which serves as a permeability barrier, has achieved long-term interest.[6-8,13] Such "Trojan horse" antibiotics are largely inspired by the sideromycins,[11,12] a family of siderophore-antibiotic conjugates produced by the soil bacterium *Streptomyces*, and by early observations that catechol-modified β-lactams were recognized by the iron-uptake machinery of Gram-negative microbes.[43-46] Significant efforts have been made to prepare and characterize synthetic siderophore-antibiotic conjugates with the goal of targeting drug-resistant Gram-negative pathogens.[13,14] Timely examples of siderophore-antibiotic conjugates with antimicrobial activity include a mycobactin-artemisinin conjugate that kills *Mycobacterium tuberculosis* and *Plasmodium falciparum*,[82] and amoxicillin/ampicillin-appended tripodal triscatecholates that exhibit potent antipseudomonal activity relative to the parent β-lactam antibiotics.[49] One bottleneck with this general approach, and using siderophores in other applications, is that few synthetically tractable and modifiable native siderophores are available. DFO B and pyoverdine, which are readily obtained commercially (DFO B) or from bacterial cultures (pyoverdines), provide free amino groups useful for conjugation and are most commonly derivatized for application-based work.[18] Syntheses of modified pyochelin,[15] petrobactin,[19] and mycobactin[82,83] platforms that house functional groups amenable to site-specific elaboration have been reported, and these scaffolds are important contributions to the toolkit of siderophores that can be modified without compromising Fe(III) coordination in addition to recognition by siderophore-binding proteins. The syntheses described in this work provide enterobactin with a functional handle for versatile chemical modifications,

and will allow strategic use of this canonical siderophore in a multitude of chemical biology and biotechnology initiatives.

Unanswered questions regarding the antibacterial activity and fate of reported synthetic siderophore-antibiotic conjugates exist. Whether a given conjugate is actively transported into the bacterial cell is oftentimes unclear. Because FepA recognizes relatively large biomolecules including MccE492m (84-aa) and colicin B (324-aa), it is tempting to predict that FepA may accommodate almost any cargo appended to an enterobactin or catecholate platform. The results presented in this work challenge this notion and indicate that cargo size is an important and species-specific parameter. Our assays indicate that *P. aeruginosa* PAO1 has a greater capacity to import enterobactin-cargo conjugates than *E. coli* ATCC 33475. It will be interesting to determine the cargo scope of other *E. coli* strains and bacterial species that utilize enterobactin for iron acquisition, and understand the molecular and physiological basis for such variations. Colicins are largely α-helical[40] and MccE492m shares some sequence homology with colicins.[84] It is likely that some enterobactin receptors have decreased propensity to transport synthetic small molecules or natural products with less structural malleability (i.e. vancomycin) than an α-helical peptide.

The mechanisms of iron release from siderophores, which vary tremendously for the myriad of siderophores produced by different bacterial species, are another important consideration in siderophore-cargo conjugate design. Guided by studies of chiral recognition in enterobactin transport, which demonstrated that D-Ent is transported into *E. coli* but cannot be hydrolyzed by Fes,[71] we designed the monofunctionalized D-Ent scaffolds to probe cytosolic delivery. This design feature prevents esterase-catalyzed iron release from enterobactin-based conjugates in the cytoplasm and may have practical utility. From the standpoint of drug delivery, a tug-of-war may result from utilizing an iron-supplying siderophore that confers a growth advantage for delivering a toxic payload to a bacterial cell, and preventing iron release may be beneficial. In other applications, siderophore-fluorophore conjugates are of interest for bacterial

detection and diagnostics, and Fe(III) binding to and release from the siderophore will likely influence the photophysical properties of such molecules.

In summary, these investigations reveal that the enterobactin transport machineries of *E. coli* (e.g. FepABCDG and TonB-ExbB-ExbD) and *P. aeruginosa* will deliver enterobactin-modified cargo to the Gram-negative cytoplasm. Moreover, the preparative work affords a new siderophore platform amenable to synthetic elaboration and an entry route for employing the native enterobactin scaffold in a multitude of application-based initiatives that include intracellular cargo delivery, iron sensing, siderophore labeling, protein and pathogen detection, and therapeutic development.

Acknowledgements. The Searle Scholars Program (Kinship Foundation), the Department of Chemistry and the Undergraduate Research Opportunities Program (UROP) at MIT, and the Amgen Scholars Program (J.L.B) are gratefully acknowledged for financial support. We thank Professor Keith Poole for providing the *Pseudomonas aeruginosa* strains employed in this work, Professor Klaus Hantke for providing the *E. coli* H1178 (*fepA*-) strain, Professor Stephen J. Lippard for use an IR spectrophotometer and a melting point apparatus, and Dr. Andrew Wommack for carefully proof-reading the manuscript. *E. coli* K-12 JW0576 was obtained from the Keio Collection.[85] NMR instrumentation maintained by the MIT DCIF is supported by NSF grants CHE-9808061 and DBI-9729592.

Supporting Information. Syntheses and characterization of **14-18** and **26-28**, general liquid chromatography, mass spectrometry and microbiology methods, summary of enterobactin-cargo conjugate characterization (Table S1), summary of bacterial strains and sources (Table S2), structure of MccE492m (Figure S1), HPLC traces for the purified conjugates (Figures S2-S11), optical absorption spectra (Figures S12-S14), growth recovery assays (Figures S15-19), ^{1}H and ^{13}C NMR spectra, and IR spectroscopic data. This material is available free of charge via the Internet at http://pubs.acs.org.

References

1. Hider, R. C.; Kong, X. *Nat. Prod. Rep.* **2010,** *27*, 637-657.
2. Miethke, M.; Marahiel, M. A. *Microbiol. Mol. Biol. Rev.* **2007,** *71*, 413-451.
3. Rajkumar, M.; Ae, N.; Prasad, M. N. V.; Freitas, H. *TRENDS Biotechnol.* **2010,** *28*, 142-149.
4. Bernhardt, P. V. *Dalton Trans.* **2007,** 3214-3220.
5. Manning, T.; Kean, G.; Thomas, J.; Thomas, K.; Corbitt, M.; Gosnell, D.; Ware, R.; Fulp, S.; Jarrard, J.; Phillips, D. *Curr. Med. Chem.* **2009,** *16*, 2416-2429.
6. Miller, M. J., *Chem. Rev.* **1989,** *89*, 1563-1579.
7. Roosenberg, J. M., II; Lin, Y.-M.; Lu, Y.; Miller, M. J. *Curr. Med. Chem.* **2000,** *7*, 159-197.
8. Budzikiewicz, H. *Curr. Top. Med. Chem.* **2001,** *1*, 73-82.
9. Ballouche, M.; Cornelis, P.; Baysse, C. *Recent Pat. Anti-infect. Drug Discovery* **2009,** *4*, 190-205.
10. Möllmann, U.; Heinisch, L.; Bauernfeind, A.; Köhler, T.; Ankel-Fuchs, D. *Biometals* **2009,** *22*, 615-624.
11. Braun, V.; Pramanik, A.; Gwinner, T.; Köberle, M.; Bohn, E. *Biometals* **2009,** *22*, 3-13.
12. Braun, V., *Drug Resist. Update* **1999,** *2*, 363-369.
13. Ji, C.; Juárez-Hernández, R. E.; Miller, M. J. *Future Med. Chem.* **2012,** *4*, 297-313.
14. Miller, M. J.; Zhu, H.; Xu, Y.; Wu, C.; Walz, A. J.; Vergne, A.; Roosenberg, J. M.; Moraski, G.; Minnick, A. A.; McKee-Dolence, J.; Hu, J.; Fennell, K.; Kurt Dolence, E.; Dong, L.; Franzblau, S.; Malouin, F.; Möllmann, U. *Biometals* **2009,** *22*, 61-75.
15. Nöel, S.; Guillon, L.; Schalk, I. J.; Mislin, G. L. A. *Org. Lett.* **2011,** *13*, 844-847.
16. Espósito, B. P.; Epsztejn, S.; Breuer, W.; Cabantchik, Z. I. *Anal. Biochem.* **2002,** *304*, 1-18.
17. Lam, C. K. S. C. C.; Jickells, T. D.; Richardson, D. J.; Russell, D. A. *Anal. Chem.* **2006,** *78*, 5040-5045.

18. Zheng, T.; Nolan, E. M. *Metallomics* **2012,** *4*, 866-880.

19. Bugdahn, N.; Peuckert, F.; Albrecht, A. G.; Miethke, M.; Marahiel, M. A.; Oberthür, M., *Angew. Chem. Int. Ed.* **2010,** *49*, 10210-10213.

20. Doorneweerd, D. D.; Henne, W. A.; Reifenberger, R. G.; Low, P. S. *Langmuir* **2010,** *26*, 15424-15429.

21. Kim, Y.; Lyvers, D. P.; Wei, A.; Reifenberger, R. G.; Low, P. S. *Lab Chip* **2012,** *12*, 971-976.

22. Raymond, K. N.; Dertz, E. A.; Kim, S. S. *Proc. Natl. Acad. Sci. U. S. A.* **2003,** *100*, 3584-3588.

23. Crosa, J. H.; Walsh, C. T. *Microbiol. Mol. Biol. Rev.* **2002,** *66*, 223-249.

24. Loomis, L. D.; Raymond, K. N. *Inorg. Chem.* **1991,** *30*, 906-911.

25. Buchanan, S. K.; Smith, B. S.; Venkatramani, L.; Xia, D.; Esser, L.; Palnitkar, M.; Chakraborty, R.; van der Helm, D.; Deisenhofer, J. *Nat. Struct. Biol.* **1999,** *6*, 56-63.

26. Newton, S. M. C.; Igo, J. D.; Scott, D. C.; Klebba, P. E. *Mol. Microbiol.* **1999,** *32*, 1153-1165.

27. Stephens, D. L.; Choe, M. D.; Earhart, C. F. *Microbiology-UK* **1995,** *141*, 1647-1654.

28. Chenault, S. S.; Earhart, C. F. *Mol. Microbiol.* **1991,** *5*, 1405-1413.

29. Shea, C. M.; Mcintosh, M. A. *Mol. Microbiol.* **1991,** *5*, 1415-1428.

30. Chakraborty, R.; Storey, E.; van der Helm, D. *Biometals* **2007,** *20*, 263-274.

31. Krewulak, K. D.; Vogel, H. J. *Biochim. Biophys. Acta.* **2008,** *1778*, 1781-1804.

32. Chu, B. C.; Garcia-Herrero, A.; Johanson, T. H.; Krewulak, K. D.; Lau, C. K.; Peacock, R. S.; Slavinskaya, Z.; Vogel, H. J. *Biometals* **2010,** *23*, 601-611.

33. Lin, H.; Fischbach, M. A.; Liu, D. R.; Walsh, C. T. *J. Am. Chem. Soc.* **2005,** *127*, 11075-11084.

34. Miethke, M.; Hou, J.; Marahiel, M. A. *Biochemistry* **2011,** *50*, 10951-10964.

35. Bäumler, A. J.; Norris, T. L.; Lasco, T.; Voigt, W.; Reissbrodt, R.; Rabsch, W.; Heffron, F., *J. Bacteriol.* **1998,** *180*, 1446-1453.

36. Lagos, R.; Baeza, M.; Corsini, G.; Hetz, C.; Strahsburger, E.; Castillo, J. A.; Vergara, C.; Monasterio, O. *Mol. Microbiol.* **2001,** *42*, 229-243.

37. Nolan, E. M.; Fischbach, M. A.; Koglin, A.; Walsh, C. T. *J. Am. Chem. Soc.* **2007,** *129*, 14336-14347.

38. Fischbach, M. A.; Lin, H. N.; Liu, D. R.; Walsh, C. T., *Proc. Natl. Acad. Sci. U. S. A.* **2005,** *102*, 571-576.

39. Müller, S.; Valdebenito, M.; Hantke, K. *Biometals* **2009,** *22*, 691-695.

40. Cao, Z.; Klebba, P. E. *Biochimie* **2002,** *84*, 399-412.

41. Lagos, R.; Tello, M.; Mercado, G.; Garciá, V.; Monasterio, O. *Curr. Pharm. Biotechnol.* **2009,** *10*, 74-85.

42. Rabsch, W.; Ma, L.; Wiley, G.; Najar, F. Z.; Kaserer, W.; Schuerch, D. W.; Klebba, J. E.; Roe, B. A.; Gomez, J. A. L.; Schallmey, M.; Newton, S. M. C.; Klebba, P. E. *J. Bacteriol.* **2007,** *189*, 5658-5674.

43. Katsu, K.; Kitoh, K.; Inoue, M.; Mitsuhashi, S. *Antimicrob. Agents Chemother.* **1982,** *22*, 181-185.

44. Watanabe, N.-A.; Nagasu, T.; Katsu, K.; Kitoh, K. *Antimicrob. Agents Chemother.* **1987,** *31*, 497-504.

45. Nakagawa, S.; Sanada, M.; Matsuda, K.; Hazumi, N.; Tanaka, N. *Antimicrob. Agents Chemother.* **1987,** *31*, 1100-1105.

46. Hashizume, T.; Sanada, M.; Nakagawa, S.; Tanaka, N. *J. Antibiot.* **1990,** *43*, 1617-1620.

47. Möllmann, U.; Ghosh, A.; Dolence, E. K.; Dolence, J. A.; Ghosh, M.; Miller, M. J.; Reissbrodt, R. *Biometals* **1998,** *11*, 1-12.

48. Mckee, J. A.; Sharma, S. K.; Miller, M. J. *Bioconjugate Chem.* **1991,** *2*, 281-291.

49. Ji, C.; Miller, P. A.; Miller, M. J. *J. Am. Chem. Soc.* **2012,** *134*, 9898-9901.

50. Diarra, M. S.; Lavoie, M. C.; Jacques, M.; Darwish, I.; Dolence, E. K.; Dolence, J. A.; Ghosh, A.; Ghosh, M.; Miller, M. J.; Malouin, F. *Antimicrob. Agents Chemother.* **1996,** *40*, 2610-2617.

51. Ghosh, A.; Ghosh, M.; Niu, C.; Malouin, F.; Möllmann, U.; Miller, M. J. *Chem. Biol.* **1996,** *3*, 1011-9.

52. Corey, E. J.; Bhattacharyya, S. *Tetrahedron Lett.* **1977,** *45*, 3919-3922.

53. Rastetter, W. H.; Erickson, T. J.; Venuti, M. C. *J. Org. Chem.* **1981,** *46*, 3579-3590.

54. Shanzer, A.; Libman, J. *J. Chem. Soc., Chem. Commun.* **1983,** *15*, 846-847.

55. Ramirez, R. J. A.; Karamanukyan, L.; Ortiz, S.; Gutierrez, C. G. *Tetrahedron Lett.* **1997,** *38*, 749-752.

56. Marinez, E. R.; Salmassian, E. K.; Lau, T. T.; Gutierrez, C. G. *J. Org. Chem.* **1996,** *61*, 3548-3550.

57. Rodgers, S. J.; Lee, C.-W.; Ng, C. Y.; Raymond, K. N. *Inorg. Chem.* **1987,** *26*, 1622-1625.

58. Tor, Y.; Libman, J.; Shanzer, A.; Felder, C. E.; Lifson, S. *J. Am. Chem. Soc.* **1992,** *114*, 6661-6671.

59. Ecker, D. J.; Loomis, L. D.; Cass, M. E.; Raymond, K. N. *J. Am. Chem. Soc.* **1988,** *110*, 2457-2464.

60. Stack, T. D. P.; Hou, Z.; Raymond, K. N. *J. Am. Chem. Soc.* **1993,** *115*, 6466-6467.

61. Yu, X.; Dai, Y.; Yang, T.; Gagné, M. R.; Gong, H. *Tetrahedron* **2011,** *67*, 144-151.

62. Gardner, R. A.; Kinkade, R.; Wang, C.; Phanstiel IV, O. *J. Org. Chem.* **2004,** *69*, 3530-3537.

63. Arnusch, C. J.; Bonvin, A. M. J. J.; Verel, A. M.; Jansen, W. T. M.; Liskamp, R. M. J.; de Kruijff, B.; Pieters, R. J.; Breukink, E. *Biochemistry* **2008,** *47*, 12661-12663.

64. Luo, M.; Lin, H.; Fischbach, M. A.; Liu, D. R.; Walsh, C. T.; Groves, J. T. *ACS Chem. Biol.* **2006,** *1*, 29-32.

65. Thomas, X.; Destoumieux-Garzón, D.; Peduzzi, J.; Afonso, C.; Blond, A.; Birlirakis, N.; Goulard, C.; Dubost, L.; Thai, R.; Tabet, J.-C.; Rebuffat, S., *J. Biol. Chem.* **2004,** *279*, 28233-28242.

66. Abergel, R. J.; Zawadzka, A. M.; Hoette, T. M.; Raymond, K. N. *J. Am. Chem. Soc.* **2009,** *131*, 12682-12692.

67. Zheng, T.; Nolan, E. *Unpublished results*.

68. Hubbard, B. K.; Walsh, C. T. *Angew. Chem. Int. Ed.* **2003,** *42*, 730-765.

69. Lawson, M. C.; Shoemaker, R.; Hoth, K. B.; Bowman, C. N.; Anseth, K. S. *Biomacromolecules* **2009,** *10*, 2221-2234.

70. Scarrow, R. C.; Ecker, D. J.; Ng, C.; Liu, S.; Raymond, K. N. *Inorg. Chem.* **1991,** *30*, 900-906.

71. Wayne, R.; Frick, K.; Neilands, J. B. *J. Bacteriol.* **1976,** *126*, 7-12.

72. Mossialos, D.; Amoutzias, G. D. *Future Microbiol.* **2007,** *2*, 387-395.

73. Cornelis, P. *App. Microbiol. Biotechnol.* **2010,** *86*, 1637-1645.

74. Poole, K.; Young, L.; Neshat, S. *J. Bacteriol.* **1990,** *172*, 6991-6996.

75. Dean, C. R.; Neshat, S.; Poole, K. *J. Bacteriol.* **1996,** *178*, 5361-5369.

76. Ghysels, B.; Ochsner, U.; Möllman, U.; Heinisch, L.; Vasil, M.; Cornelis, P.; Matthijs, S. *FEMS Microbiol. Lett.* **2005,** *246* (2), 167-174.

77. Collin, F.; Karkare, S.; Maxwell, A. *App. Microbiol. Biotechnol.* **2011,** *92*, 479-497.

78. Hennard, C.; Truong, Q. C.; Desnottes, J.-F.; Paris, J. M.; Moreau, N. J.; Abdallah, M. A. *J. Med. Chem.* **2001,** *44*, 2139-2151.

79. Rivault, F.; Liébert, C.; Burger, A.; Hoegy, F.; Abdallah, M. A.; Schalk, I. J.; Mislin, G. L. A. *Bioorg. Med. Chem. Lett.* **2007,** *17*, 640-644.

80. Nöel, S.; Gasser, V.; Pesset, B.; Hoegy, F.; Rognan, D.; Schalk, I. J.; Mislin, G. L. A. *Org. Biomol. Chem.* **2011,** *9* (24), 8288-8300.

81. Ji, C.; Miller, M. J. *Bioorg. Med. Chem.* **2012,** *20*, 3828-3836.

82. Miller, M. J.; Walz, A. J.; Zhu, H.; Wu, C.; Moraski, G.; Möllmann, U.; Tristani, E. M.; Crumbliss, A. L.; Ferdig, M. T.; Checkley, L.; Edwards, R. L.; Boshoff, H. I. *J. Am. Chem. Soc.* **2011,** *133*, 2076-2079.

83. Xu, Y.; Miller, M. J. *J. Org. Chem.* **1998,** *63*, 4314-4322.

84. Pons, A.-M.; Zorn, N.; Vignon, D.; Delalande, F.; Dorsselaer, A. V.; Cottenceau, G. *Antimicrob. Agents Chemother.* **2002**, *46*, 229-230.

85. Baba, T.; Ara, T.; Hasegawa, M.; Takai, Y.; Okumura, Y.; Baba, M.; Datsenko, K. A.; Tomita, M.; Wanner, B. L.; Mori, H., *Mol. Sys. Biol.* **2006**, 2006.0008.

TOC Graphic

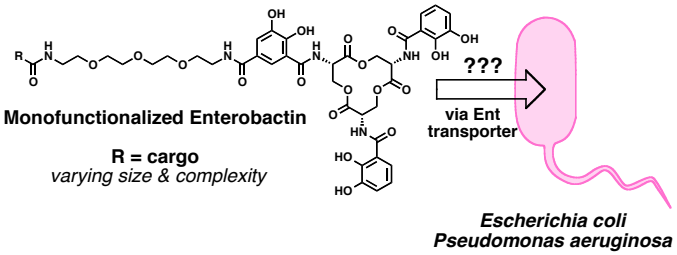
???
via Ent
transporter
Monofunctionalized Enterobactin
R = cargo
varying size & complexity
Escherichia coli
Pseudomonas aeruginosa